

PHOTOLUMINESCENCE STUDY OF Ge-IMPLANTED GaSe AND InSe  
SINGLE CRYSTALS GROWN BY BRIDGMAN METHOD

A THESIS SUBMITTED TO  
THE GRADUATE SCHOOL OF NATURAL AND APPLIED SCIENCES  
OF  
MIDDLE EAST TECHNICAL UNIVERSITY

By

SEDA BILGI

IN PARTIAL FULFILLMENT OF THE REQUIREMENTS  
FOR  
THE DEGREE OF MASTER OF SCIENCE  
IN  
PHYSICS

AUGUST 2006

Approval of the Graduate School of Natural and Applied Sciences

---

Prof. Dr. Canan Özgen  
Director

I certify that this thesis satisfies all the requirements as a thesis for the degree of Master of Science.

---

Prof. Dr. Sinan Bilikmen  
Head of Department

This is to certify that we have read this thesis and that in our opinion it is fully adequate, in scope and quality, as a thesis for the degree of Master of Science.

---

Prof. Dr. Raşit Turan  
Co-Supervisor

---

Prof. Dr. Bülent G. Akınoğlu  
Supervisor

**Examining Committee Members**

Prof. Dr. Çiğdem Erçelebi (METU, PHYS) \_\_\_\_\_

Prof. Dr. Bülent Akınoğlu (METU, PHYS) \_\_\_\_\_

Prof. Dr. Raşit Turan (METU, PHYS) \_\_\_\_\_

Prof. Dr. Mehmet Parlak (METU, PHYS) \_\_\_\_\_

Prof. Dr. Bahtiyar Salamov (Gazi Unv., PHYS) \_\_\_\_\_

**I hereby declare that all information in this document has been obtained and presented in accordance with academic rules and ethical conduct. I also declare that, as required by these rules and conduct, I have fully cited and referenced all material and results that are not original to this work.**

Name, Last name : Seda Bilgi

Signature :

## ABSTRACT

### PHOTOLUMINESCENCE STUDY OF Ge-IMPLANTED GaSe AND InSe SINGLE CRYSTALS GROWN BY BRIDGMAN METHOD

Bilgi, Seda

M.Sc., Department of Physics

Supervisor: Prof. Dr. Bülent G. Akınoğlu

Co-Supervisor: Prof. Dr. Raşit Turan

August 2006, 90 sayfa

In this study, photoluminescence properties of as grown, Ge implanted GaSe and InSe crystals with doses  $10^{13}$ ,  $10^{14}$ , and  $10^{15}$  ions/cm<sup>2</sup> and  $10^{15}$  ions/cm<sup>2</sup> Ge implanted and annealed GaSe and InSe single crystals grown by using 3-zone vertical Bridgman-Stockbarger system have been studied by photoluminescence spectroscopy (PL). PL spectra of as grown and implanted GaSe samples with three different doses have been studied in the ranges within the wavelength interval 570-850 nm and in the temperature ranges between 21 and 110 K. Temperature dependencies of all observed bands revealed that the peak with highest energy has excitonic origin and most of the others originate from donor-acceptor pair recombination.

For GaSe samples implanted with  $10^{13}$  and  $10^{15}$  ions/cm<sup>2</sup> Ge, PL spectra exhibited four emission bands while for as grown and the sample implanted with  $10^{14}$  ions/cm<sup>2</sup>

Ge had three bands. Variations of emission peaks were studied as a function of temperature. It was observed that centers of all bands shifted towards red continuously with temperature. The intensities of the emission peaks showed similarities with those obtained from as grown,  $10^{13}$  and  $10^{14}$  ions/cm<sup>2</sup> Ge implanted GaSe while the peak intensities of the sample implanted with  $10^{15}$  ions/cm<sup>2</sup> Ge decreased with the temperature continuously.

Using the temperature variation of the peak intensities and peak energy values activation energies were obtained and these results revealed that the two bands with low wavelength to be excitonic origin for the implanted samples with the doses  $10^{13}$  and  $10^{15}$  ions/cm<sup>2</sup> Ge. Similar results were obtained for the implanted with  $10^{15}$  ions/cm<sup>2</sup> Ge and annealed sample. The other two peaks observed for these samples were attributed to donor acceptor pair transitions.

In addition, direct band gaps were found to be 2.12 eV at 32 K for as grown, 2.121 eV at 25 K for  $10^{13}$  ions/cm<sup>2</sup> Ge implanted, 2.121 eV at 21 K for  $10^{14}$  ions/cm<sup>2</sup> Ge implanted, 2.124 eV at 33 K for  $10^{15}$  ions/cm<sup>2</sup> Ge implanted GaSe samples and lastly 2.113 eV at 28 K for  $10^{15}$  ions/cm<sup>2</sup> Ge implanted and annealed GaSe.

PL spectra of as grown,  $10^{13}$ ,  $10^{14}$ ,  $10^{15}$  ions/cm<sup>2</sup> Ge implanted, and  $10^{15}$  ion/cm<sup>2</sup> Ge implanted and annealed InSe samples were also obtained at 20 K. Two broad bands were observed in the spectrum of all InSe crystals and considered to be due to impurity levels within the materials.

Keywords: Bridgman technique, GaSe, InSe, ion implantation, photoluminescence spectroscopy.

## ÖZ

### BRİDGMAN YÖNTEMİ İLE BÜYÜTÜLEN Ge-EKİLMİŞ GaSe VE InSe TEK KRİSTALLERİNİN FOTOLÜMİNESANS ÇALIŞMASI

Bilgi, Seda

Yüksek Lisans, Fizik Bölümü

Tez Yöneticisi: Prof. Dr. Bülent G. Akınoğlu

Ortak-Tez Yöneticisi: Prof. Dr. Raşit Turan

Ağustos 2006, 90 sayfa

Bu çalışmada, 3-bölgeli dikey Bridgman-Stockbarger düzeneği ile büyütülmüş katkılanmamış,  $10^{13}$ ,  $10^{14}$  ve  $10^{15}$  iyon/cm<sup>2</sup> dozlarıyla Ge ekilmiş ve  $10^{15}$  iyon/cm<sup>2</sup> Ge ekilmiş ve tavllanmış GaSe ve InSe tek kristallerin fotolüminesans spektroskopisi incelenmiştir. Katkılanmamış ve üç farklı dozda Ge-ekilmiş GaSe ve InSe örneklerinin fotolüminesansı 570-850 nm dalga boyu ve 21 ile 110 K sıcaklık aralıklarında çalışılmıştır. Bütün gözlenen piklerin sıcaklık bağımlılıkları en yüksek enerjiye sahip pikin eksitonik kökenli olduğunu ve diğer bantların büyük kısmının verici-alıcı çifti rekombinasyonundan kaynaklandığını ortaya çıkarmıştır.

$10^{13}$  ve  $10^{15}$  iyon/cm<sup>2</sup> Ge ekilmiş GaSe örneklerinin fotolüminesans spektrumları dört emisyon bandı gösterirken ekilmemiş ve  $10^{14}$  iyon/cm<sup>2</sup> Ge ekilmiş örnekler için fotolüminesans spektrumu üç bant içermektedir. Emisyon bantlarının değişimi sıcaklığın fonksiyonu olarak çalışılmıştır. Katkılanmamış,  $10^{13}$  ve  $10^{14}$  iyon/cm<sup>2</sup> Ge

ekilmiş GaSe için emisyon piklerinin şiddetleri benzerlikler gösterirken,  $10^{15}$  iyon/cm<sup>2</sup> Ge ekilmiş örneğin pik şiddeti sıcaklıkla beraber düzenli olarak düşmüştür. Pik şiddetlerinin ve enerji değerlerinin sıcaklıkla beraber değişimini kullanarak aktivasyon enerjileri elde edilmiştir ve bu sonuçlar  $10^{13}$  ve  $10^{15}$  iyon/cm<sup>2</sup> dozlarında Ge ekilmiş örnekler için düşük dalga boylu iki bandın eksitonik kökenli olduğunu ortaya çıkarmıştır. Benzer sonuçlar  $10^{15}$  iyon/cm<sup>2</sup> Ge ekilmiş ve tavllanmış örnek içinde elde edilmiştir. Bu örneklerde gözlenen diğer iki pik verici-alıcı çifti rekombinasyonuna yorulmuştur.

Ek olarak, direk yasak enerji bantları ekilmemiş örnek için 32 K' de 2.12 eV,  $10^{13}$  iyon/cm<sup>2</sup> Ge ekilmiş için 25 K' de 2.121 eV,  $10^{14}$  iyon/cm<sup>2</sup> Ge ekilmiş için 21 K' de 2.121 eV,  $10^{15}$  iyon/cm<sup>2</sup> Ge ekilmiş GaSe örneği için 33 K' de 2.124 eV ve son olarak  $10^{15}$  iyon/cm<sup>2</sup> Ge ekilmiş ve tavllanmış örnekte 28 K' de 2.113 eV bulunmuştur.

Katkılanmamış,  $10^{13}$ ,  $10^{14}$ ,  $10^{15}$  iyon/cm<sup>2</sup> Ge ekilmiş ve  $10^{15}$  iyon/cm<sup>2</sup> Ge ekilmiş ve tavllanmış InSe örneklerinin fotoluminesans spektrumları 20 K'de elde edilmiştir. Bütün InSe kristallerinin spektrumunda iki geniş bant elde edilmiş ve bunların malzemedeki safsızlık düzeylerinden kaynaklandığı düşünülmüştür.

Anahtar Kelimeler: Bridgman tekniği, GaSe, InSe, iyon ekme, fotoluminesans spektroskopisi.

*To My Parents, My Brother,  
and My Twin Sister*

## ACKNOWLEDGEMENTS

First of all, I would like to express my thanks to my supervisor, Prof. Dr. Bülent G. Akinođlu, for his encouragement, understanding, support and guidance throughout this study. In addition, I would like to present my sincere thanks to co-supervisor Prof. Dr. Rařıt Turan for providing his laboratory opportunity, friendly attitude and encouragement during the investigation. Also, I wish to thank his group members; Uđur Serincan, Mustafa Kulakçı and Ayře Seyhan for their helps during the ion implantation and in the beginning stage of the photoluminescence measurements. I also should thank my roommate Hazbullah Karaađaç for his supportive manner and great helps with patience whenever I need in difficult moments. In addition, I would like to express my thanks to Prof. Dr. Nizami Gasanly for his discussions with helpful manner and Kadir Gökřen for his helps. I also would like to thank my committee members Prof. Dr. ıđdem Erelebi, Prof. Dr. Mehmet Parlak, and Prof. Dr. Bahtiyar Salamov for their time and comments.

My deepest thanks go to each member of my lovely family for their continuous supports and encouragements, great understanding, friendly attitudes and their endless love to achieve my goals at every stage of my life. I am very lucky to have such a perfect family. Without them I would not complete this study.

## TABLE OF CONTENTS

PLAGIARISM .....	iii
ABSTRACT .....	iv
ÖZ .....	vi
DEDICATION .....	viii
ACKNOWLEDGMENTS .....	ix
TABLE OF CONTENTS .....	x
LIST OF TABLES .....	xii
LIST OF FIGURES .....	xiii
CHAPTERS	
1. INTRODUCTION .....	1
1.1 Crystals and Electronic Band Structures of GaSe and InSe.....	3
1.2 Previous Studies .....	7
1.2.1 Previous Studies About PL Properties of GaSe .....	8
1.2.2 Previous Studies About PL Properties of InSe .....	14
1.3 Present Study.....	19
2. THEORETICAL CONSIDERATIONS .....	21
2.1 Introduction .....	21
2.2 Crystal Growth .....	21
2.3 Ion Implantation and Annealing .....	23
2.4 Luminescence .....	26
2.5 Photoluminescence Spectroscopy .....	27
2.5.1 Recombination Mechanisms .....	28
2.5.1.1 Band to Band Transition .....	30

2.5.1.2	Free to Bound Transitions .....	32
2.5.1.3	Donor Acceptor Pair Transition .....	32
2.5.1.4	Excitonic Transitions .....	33
2.6	Effects of Variations in Laser Power and Temperature on Photoluminescence Intensity .....	35
2.7	Recombination Rate and Carrier Lifetime .....	37
3.	EXPERIMENTAL TECHNIQUES .....	41
3.1	Introduction .....	41
3.2	Crystal Growth by Bridgman-Stockbarger Technique .....	41
3.3	Ion Implantation and Annealing Processes.....	46
3.4	Photoluminescence Measurements.....	48
3.4.1	Photoluminescence System .....	48
3.4.2	Measurements by PL System .....	52
4.	RESULTS AND DISCUSSIONS .....	54
4.1	Introduction .....	54
4.2	PL Analysis of As Grown GaSe .....	54
4.3	PL Analysis of $10^{13}$ ions/cm <sup>2</sup> Ge Implanted GaSe .....	60
4.5	PL Analysis of $10^{14}$ ions/cm <sup>2</sup> Ge Implanted GaSe .....	64
4.5	PL Analysis of $10^{15}$ ions/cm <sup>2</sup> Ge Implanted GaSe .....	68
4.6	PL Analysis of $10^{15}$ ions/cm <sup>2</sup> Ge Implanted and annealed GaSe .	72
4.7	Comparison of Results Obtained From As Grown and Implanted Samples .....	77
4.8	PL Analysis of InSe Crystals .....	80
5.	CONCLUSION .....	82
	REFERENCES .....	85

## LIST OF TABLES

### TABLE

1.1	The interatomic distances in the GaSe polytypes.....	5
1.2	The interatomic distances in the $\gamma$ - type InSe.....	6
1.3	Ten of the previously observed peaks in the PL spectra of GaSe.....	18
1.4	Previously observed PL bands in InSe single crystals.....	19
3.1	Samples used in PL measurements and their donated names.....	48
3.2	Groove spacing and peak efficiency for each grating .....	51
5.1	Obtained PL bands for GaSe samples in this study .....	83

## LIST OF FIGURES

### FIGURE

1.1	Structure of one of the four-fold layers of GaSe and InSe [5] (Gallium (indium) atoms are represented by full circles while the selenium atoms are represented by open circles.) .....	4
1.2	Polytypes of GaSe [2]; (a) 2H- $\epsilon$ polytype, (b) 2H- $\beta$ polytype, (c) 3R- $\gamma$ polytype, (d) 4H- $\delta$ polytype.....	5
1.3	The band structure of GaSe .....	6
1.4	The band structure of GaSe .....	7
2.1	Schematic representation of the ion range $R$ and projected range $R_p$ ..	25
2.2	Damage resulted from (a) light ions and (b) heavy ions .....	25
2.3	Schematic showing of photoluminescence processes [3]. (a) The creation of an electron hole pair by optical excitation. (b) Releasing energy of the promoted electron in the conduction band (c) The recombination of an electron in the conduction band and a hole in the valence band resulting in the emission of light .....	28
2.4	The most common radiative recombination mechanisms. (A) Band to band transition, (B) donor to valance band transition (C) conduction band to acceptor transition, (D) donor to acceptor transition, (E) free exciton recombination, and (F) bound-exciton recombination .....	30
2.5	Schematic representation of radiative band to band recombination for a direct edge (a) and indirect edge (b) in energy-momentum space .....	31
2.6	Schematic representation of the energy levels of an exciton in a semiconductor .....	34
3.1	Some pointed bottom crucible with different diameters .....	42

3.2	Bridgman Stockbarger System in the Crystal Growth Laboratory of Physics Department at METU.....	44
3.3	Schematic diagram of furnace system and the ideal temperature distribution along the axis of a cylindrical crucible .....	45
3.4	Schematic diagram of an implantation system .....	46
3.5	Ion implantation system in METU Physics department .....	47
3.6	Photoluminescence set up in Department of Physics at METU .....	49
3.7	“CTI-Cryogenics M-22” closed-cycle helium cryostat system .....	50
3.8	Diagram representation of MS257 <sup>TM</sup> as a monochromator .....	51
3.9	The schematic representation of our PL set-up .....	53
4.1	Temperature dependence of emission spectrum obtained from GaSe-0 single crystal in the temperature range 32-85 K .....	55
4.2	Temperature dependence of the A, B, and C bands (The arrows shows the starting points of intensive thermal quenching.) .....	56
4.3	Temperature dependence of the peak energies of B and C bands (The dashed line shows the variation of direct band gap of GaSe.) .....	58
4.4	Proposed energy diagram of the impurity levels in GaSe-0 sample at 32 K .....	59
4.5	PL spectra of GaSe-1 sample a function of temperature .....	60
4.6	PL intensities of observed bands as a function of reciprocal temperature, the arrows show the starting temperatures of rapid thermal quenching .....	61
4.7	Temperature dependencies of C and D-bands peak energies for GaSe-1 sample .....	63
4.8	Proposed energy band diagram of luminescence related with impurity levels in GaSe-1 sample at 25 K .....	64
4.9	Temperature dependence of PL spectrum from GaSe-2 crystal .....	65
4.10	Temperature dependence of the peak intensity of A, B and C bands (The starting temperatures of rapid thermal quenching of the bands has been shown with arrows.) .....	66
4.11	The variation of the peak center energies with temperature .....	67
4.12	The energy band diagram indicating B and C transitions for GaSe-2 at 21 K .....	68

4.13	PL spectra of GaSe-3 as a function of temperature .....	69
4.14	Temperature dependence of the observed peaks in GaSe-3 sample ...	70
4.15	The variation of the observed impurity related peak energies with temperature in GaSe-3 sample .....	71
4.16	The proposed energy band diagram for the observed impurity related luminescence in GaSe-3 at 33 K .....	72
4.17	Temperature dependence of PL spectra obtained from GaSe-3A .....	73
4.18	The variation of PL intensity of the bands observed in GaSe-3A .....	74
4.19	Temperature dependence of the C and D band energies .....	75
4.20	The proposed energy band diagram for GaSe-3A sample at 28 K .....	76
4.21	PL spectra of unimplanted and Ge-implanted GaSe crystals at 35 K ..	78
4.22	PL spectrum of GaSe-3 and GaSe-3A samples at 35 K .....	79
4.23	PL spectrum of InSe samples at 20 K .....	80
4.24	PL spectra of InSe-3 and InSe-3A samples at 20 K .....	81

# CHAPTER I

## INTRODUCTION

In our daily life we use many semiconductor devices such as transistors, diodes and integrated circuits. We have come to rely on these devices more and more and expect increasingly better performances from them. This fact leads us to asking such questions: what is a semiconductor and why it is so important?

Materials can be categorized as conductors, insulators and semiconductors according to their current carrying abilities. The conductivities of semiconductor materials are lying between metals and insulators. There are several important properties of semiconductors: (a) their electrical conductivity generally rises with increasing temperature, (b) the conductivity of these materials can be changed strongly by introducing impurities into structure (i.e., by doping), and (c) their electrical conductivity can be altered by various external agents such as irradiation with light and excitation by thermal energy [1].

One of the main parameters that often determines the range of applications of a given semiconductor and distinguishes it from conductors and insulators is its energy band gap, defined as the forbidden energy band between the valence band and the conduction band [2]. At 0 K valence band is filled with electrons while the conduction band is empty. Energy gap is between the highest occupied state of the valence band and the lowest empty state of the conduction band. It is typically in the range between 0 and about 4 eV for semiconductors [3]. When the temperature of a

semiconductor material is increased above 0 K, some electrons in the valence band gain enough thermal energy to be excited across the band gap to the conduction band. As a result, some unoccupied states in filled valence band and some occupied levels in empty conduction band are created. The unoccupied states are called holes, which can be regarded as positive charge carriers [3].

Another important reason that semiconductors are useful in electronic devices is that their electrical properties can be greatly changed by adding controllable amounts of foreign atoms, called dopants, to the crystal. If a semiconductor contains no intentionally or unintentionally introduced impurities or lattice defects, this semiconductor material is called intrinsic semiconductor. In such materials, at temperatures above 0 K electrons in the valence band are thermally promoted to the conduction band, resulting in generation of electron-hole pairs. Since these carriers are created in pairs, electron concentration in the conduction band is equal to the hole concentration in the valence band in this type of material [3]. If the dopants are added deliberately into a semiconductor crystal, this material is named as an extrinsic semiconductor. Depending on introduced dopant atom, the dominant charge carrier in the material will be either holes or electrons. There are two type of doped semiconductors. If dopant atoms provide extra electrons to the lattice (donors), these semiconductors are called n-type. The energy levels of the extra electrons lie just below the conduction band and named as donor levels. Also, doped atoms can accept electrons from the lattice in order to complete atomic bonding. In this case, these semiconductors are called p-type. Since in p-type materials, added impurities capture electrons and supply holes in the valence band, they are called acceptor atoms. The energy levels for the holes are located just above the valence band and are termed as acceptor levels [4].

According to number of different atom made up of semiconductors, they can be classified in two general groups. These are elemental and compound semiconductors [5]. Elemental semiconductors consist of single species of atoms. Semiconductor materials found in column IV such as silicon, germanium and diamond are three of

the important elemental semiconductors. In addition, group III element boron, group V material phosphorus, and group VI elements such as sulphur, selenium and tellurium are some elements showing semiconducting behaviour. Semiconductors formed special combinations of pure elemental semiconductors are called compound semiconductors. Such semiconductors are named according to the column number of the combined semiconducting elements. Some of these compounds includes II-VI semiconductors such as CdS, CdSe and ZnSe, III-V compounds such as GaAs and InSb, IV-VI compounds such as PbS and PbTe, and III-VI compounds such as GaSe and InSe [2].

The scope of the thesis is mainly to study the photoluminescence (PL) spectroscopy of layered structures GaSe and InSe which are important and interesting materials for their possible optoelectronic applications and due to their high anisotropy. We carried out a systematic experimental work on the photoluminescence properties of as grown and Ge implanted compound semiconductors GaSe and InSe grown in the Crystal Growth Laboratory of Physics Department, METU.

## **1.1 Crystal and Electronic Band Structures of GaSe and InSe**

GaSe and InSe, which are the members of the group III-VI, are two of semiconductors which crystallize in layered structure [6]. These layered compounds are built up of multiple layers (i.e. sandwiches), each of which consist of two close-packed metal sheets (M) and two closed-packed chalcogen sheets (X) with the arrangement X-M-M-X [7]. In another words, four closed-packed sheets constitute one layer in the structure of GaSe and InSe crystals as it is shown in Fig.1.1. [8]. In these layered structures, the c-axis is perpendicular to the layer plane [9].

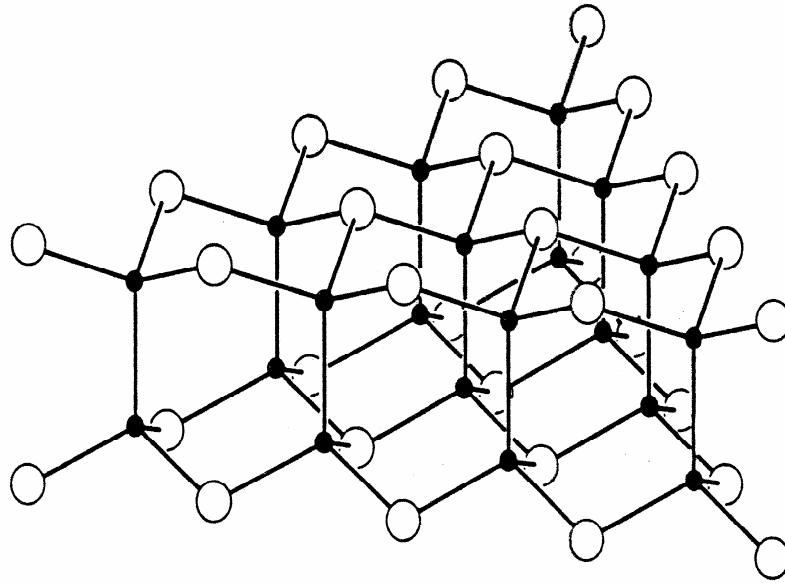


Fig.1.1. Structure of one of the four-fold layers of GaSe and InSe [10] (Gallium (indium) atoms are represented by full circles while the selenium atoms are represented by open circles.)

The bondings within the sheets are covalent and slightly ionic, while sandwiches (i.e. four-fold layers) are bound together by weak forces such as Van der Waals with some ionic or Coulomb contribution [10, 11]. The combination of strong and weak bonds in the structure gives rise to anisotropic behaviour of the layered compounds owing to highly asymmetric charge distribution surrounding atoms [7, 12, 13].

Four various polytypes of these crystals exist depending on periodic stacking. These are  $\beta$ ,  $\epsilon$ ,  $\gamma$  and  $\delta$  [14] as shown in Fig.1.2. It has been found that GaSe usually grows in  $\epsilon$ ,  $\beta$  and  $\gamma$  structures, while InSe usually exists in  $\epsilon$  and  $\gamma$  structures [8, 14, 15]. The  $\beta$  and  $\epsilon$  structures are 2H,  $\gamma$  is 3R and  $\delta$  is 4H, where H and R stand for hexagonal and rhombohedral symmetries, respectively, and the number indicates the number of structural layers [16, 17].

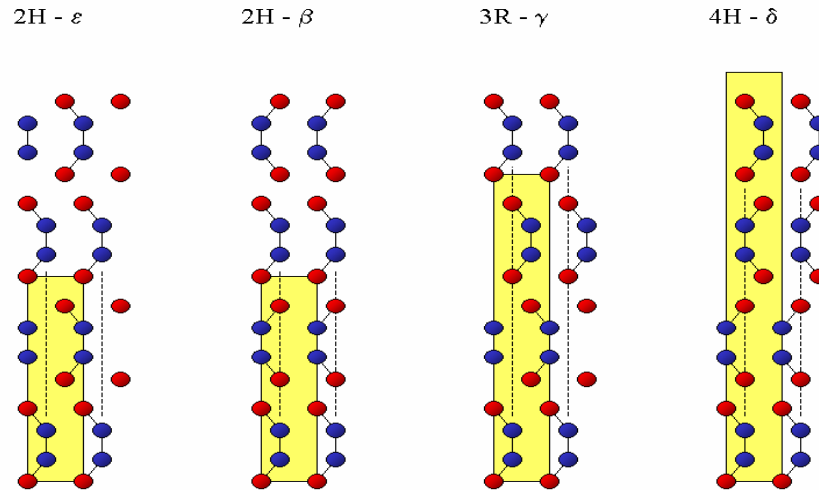


Fig.1.2. Polytypes of GaSe [7]; (a) 2H- $\epsilon$  polytype, (b) 2H- $\beta$  polytype, (c) 3R- $\gamma$  polytype, (d) 4H- $\delta$  polytype

At each polytype, interatomic distances are different from each other. Kuhn et al. [16] in their study have calculated the distances between the atoms in the layer for  $\delta$ -type GaSe crystal and in ref. [18] a table for the calculated interatomic distances for other polytypes has been given. These values are shown in Table 1.1. Because InSe has been much less investigated than GaSe, only the interatomic distances of  $\gamma$  polytype of InSe has been given in the literature as shown in Table 1.2. [15, 19].

Table 1.1. The interatomic distances in the GaSe polytypes [16, 18]

Type	Rf.	Lattice parameter a (Å)	Lattice parameter c(Å)	Se-Ga intra layer (Å)	Ga-Ga intra layer (Å)	Se-Se intra layer (Å)	Se-Se inter layer (Å)
$\beta$ 2H	18	3.755	15.94	2.600	2.231	5.101	3.596
$\epsilon$ 2H	18	3.755	15.946	2.485	2.383	4.766	3.840
$\delta$ 4H	16	3.755	23.92	2.463	2.457	4.784	3.880
$\gamma$ 3R	18	3.755	31.99	2.467	2.386	4.722	3.847

Table 1.2. The interatomic distances in the  $\gamma$ -type InSe [15, 19]

Lattice parameter $a(\text{Å}^\circ)$	Lattice parameter $c(\text{Å}^\circ)$	In-In intralayer ( $\text{Å}^\circ$ )	In-Se intralayer ( $\text{Å}^\circ$ )	In-Se intralayer ( $\text{Å}^\circ$ )	Se-Se intralayer ( $\text{Å}^\circ$ )
4.00	25.32	2.818	2.627	2.636	3.864

Electronic band structures of both materials have been studied experimentally and theoretically by many groups. McCanny et al. [16] have been found that GaSe has a direct gap with 2.1 eV and an indirect energy gap is 2.0 eV at room temperature. Moreover, in this study, indirect energy gap value for InSe has been given as 1.2 eV. Mercier et al. [20] have reported that GaSe has an indirect gap with a minimum of conduction band at M point of Brillouin zone, which is only 25 meV lower than the direct one at the  $\Gamma$  point, and a maximum of valence band at  $\Gamma$ . In another words, the indirect gap is between the top of the valence band at the  $\Gamma$  point, which is conduction minima for direct gap, and the bottom of the conduction band at the M point. In the references [21, 22] the direct gap energy in GaSe has been found as 2.01 eV at 300 K and 2.13 eV at 10 K, while the indirect one has been calculated 2.00 eV and 2.105 eV at 300 K and 10 K, respectively. The electronic band structure of GaSe given in ref. [21] is presented in Fig. 1.3.

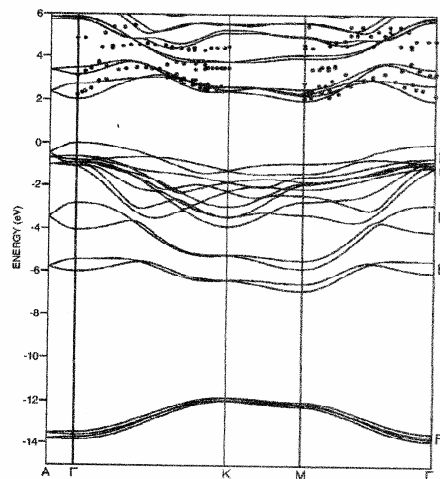


Fig.1.3. The band structure of GaSe [21]

The studies performed in order to investigate the electronic band structure of InSe display that the indirect gap is between the maximum of the valence band at the  $\Gamma$  point, and the minimum of the conduction band at the M point. In the study carried out by Camara et al. [21], at room temperature the value of the direct and indirect band gap have been found as 1.44 eV and 2.33 eV, respectively [21]. In addition, the electronic band structure of InSe shown in Fig.1.4. has been given in this study.

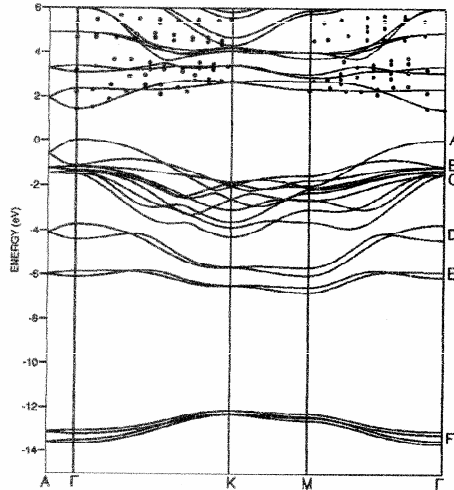


Fig.1.4. The band structure of InSe [21]

## 1.2 Literature Review

GaSe and InSe are binary layered semiconductors whose electrical, structural, and optical properties have been investigated by many researchers. In this section, only the previous studies about photoluminescence properties of them will be given. In addition, at the end of the section, tables about the observed PL lines for both of the crystals are presented.

Since GaSe and InSe layered crystals are anisotropic materials and their band structures contain both direct and indirect band gaps, their PL spectra are quite complex at low temperatures. Anisotropy in the PL spectra of as grown GaSe samples was already studied in our laboratories [23]. Another fact is that since it is difficult to grow perfect crystals, there are considerable distinctions between

experimental findings of different authors [24]. Photoluminescence properties of these materials have been widely studied by many research groups and various considerable publications have been given in the literature.

### **1.2.1 Previous Studies about PL Properties of GaSe**

One of the first investigations about the PL spectra of GaSe was conducted by J. P. Voitchovsky and A. Mercier in 1974 [25]. It was based on an investigation of PL spectra of pure and doped single crystals of GaSe, with Cu, Zn, Cd, and Sn, grown by Bridgman and transport reaction methods in the temperature range between 4.2 and 300 K using excitation intensities from  $4 \cdot 10^{-5}$  to  $3 \cdot 10^2$  kW/cm<sup>2</sup>. It was stated that the PL spectra strongly depend on temperatures below 40 K and it was observed that as the temperature was increased above this temperature, the PL spectra changed dramatically and the emission spectrum of all samples became identical independently from the amount of impurities they contain. The reason of the temperature dependence was explained by the thermal quenching of the luminescence resulting from recombination at trap states in temperatures between 20 and 40 K. At above 40 K, only the emission lines corresponding to free excitons were observed. Moreover, it was reported that the intensities of lines attributed to recombinations of free excitons and trap assisted transitions change superlinearly with the excitation intensity.

Matsumura et al. [26] have studied the dependence of PL spectra on GaSe samples obtained from different parts of the crystal ingot grown by Bridgman method. It has been stated that the emission spectra of many samples can be categorized in three types. In the spectra of the first type, type A, a broad peak at about 2.04 eV has been observed at 4.2 K. Also, the sample from which type A spectra has been obtained contain many fine cracks on its surface; therefore, the origin of the peak was explained as a radiative recombination through the state related to fine cracks. The second type spectra, type B, contained two sharp peaks at 2.095 eV and 2.088 eV and some lines at the lower energy part at the same temperature. This type of spectra has been observed in the samples prepared from the top of the grown ingot and lines

were attributed to indirect bound excitons. The third one had a free exciton line at 2.108 eV. This type of spectra, type C, has been obtained in the samples prepared from the bottom of the ingot. The reason that type B spectra were obtained in samples prepared from the top of the ingot, while type C spectra were observed in samples obtained from the bottom of the ingot has been stated as: in Bridgman method crystallization starts from the bottom and ends at the top of the ampoule, so considerable amount of impurities are contained at the top of the ingot. Moreover, it has been stated that the shape of the spectra changes with varying the exciting position on the same sample.

In 1988 Dobynde et al. [27] investigated the photoluminescence features of  $\epsilon$ -GaSe in the energy range from 2.00 to 2.12 eV at 77 K with different excitation energies and excitation intensity. Firstly, laser with 2.33 eV was directed onto the sample and PL spectrum containing two lines at 2.098 and 2.39 eV was observed. The lines were attributed to the recombination of direct free exciton and indirect free exciton, respectively. In addition, it was observed that the intensity of free excitonic line enhance with increasing excitation intensity while indirect free exciton peak decreased. Secondly, the sample was excited by a laser with 3.68 eV. In the emission spectra at this excitation energy indirect free exciton which was seen at the first excitation energy was not observed. Also, it was reported that as excitation intensity was increased, a new line at 2.069 eV begins to grow. This peak was attributed to exciton-exciton scattering.

Another study was conducted by Capozzi [24] in 1981. It was performed to investigate radiative recombination mechanisms of undoped layered crystals of  $\epsilon$ -GaSe at different temperatures and excitation levels. It was observed that with varying excitation intensity, the peak positions remained constant and relative peak intensities changed. It was possible to say that PL spectra of GaSe consist of two parts: intrinsic and extrinsic parts. This study was the analysis of only the intrinsic part of the spectra. At 80 K, he observed four emission bands at 591 nm (2.0981 eV), 597.6 nm (2.0751 eV), 609.2 nm (2.0354 eV), and 620.3 nm (1.9982 eV) and these lines were attributed to the recombination of direct free exciton, direct bound exciton indirect free exciton, and indirect bound exciton, respectively.

Capozzi et al. [28] in 1985 reported a detailed study about direct and indirect excitonic emission of p-type GaSe with crystal structure  $\epsilon$ . In the PL spectrum at 80K, five lines at 591 nm (2.098 eV), 586.8 nm (2.113 eV), 596.8 nm (2.078 eV), 609.3 nm (2.035 eV), and 619.4 nm (2.002 eV) were observed. They considered that these lines were due to the radiative recombination of direct free exciton from  $n=1$  state, transition of direct free exciton from the excited state  $n=2$ , recombination of direct bound exciton, recombination of indirect free exciton, and transition of indirect bound exciton, respectively.

In 1989, Capozzi et al. [29] performed a study of emission spectra of GaSe samples containing different degree of lattice disorder and they observed that extrinsic part of the spectrum, resulting from donor acceptor pair transitions and free to bound recombinations, increases with increasing density of the lattice disorders in the material.

Emissions related to defect levels in undoped p-type GaSe has been reported by Aydınli et al. [30]. PL spectra of undoped GaSe crystals have been measured at temperatures from 10 K up to room temperature. Two wide emission peaks located at 644 nm and 695 nm have been observed at 10 K. These two bands have been explained as recombinations through donor acceptor pairs. The first band has been attributed to transition from a deep donor level located at 0.163 eV below the conduction band to an acceptor level at 0.014 eV. The origin of other band has been given as transitions from a donor level at 0.264 eV below the conduction band to an acceptor level at 0.076 eV above the valence band.

The effects of impurity atoms on emission properties of GaSe have been widely studied. In order to compare the emission spectra of doped crystals with undoped ones, GaSe crystals have chemically doped with Zn [31], Cu [32], Cd [33], Li [34], Mn [35], Tm [36], Te [37], As [38], Bi [38], Sb [38], Ag [39], P [40], Er [41], Sn [42], Mg [43] and Cr [35]. Also, dependence of PL spectra on rare-earth dopants (Gd, Ho, and Dy) have been investigated [44].

The PL measurements with undoped and Zn doped p-type GaSe have been

performed by Shigetomi et al. in 1993 [31]. They were added Zn atoms into the growing GaSe crystal in a range from 0.005 to 0.5 at. %. In the PL spectra of Zn doped crystals, dominance of three emission bands centered at 1.75, 1.63, and 1.27 eV were observed at 77 K. The origin of peaks at 1.75 and 1.63 eV were explained as transition from the donor level at 0.37 eV below the conduction band to valence band and recombination of the electrons at the same donor level and holes at an acceptor level located 0.12 eV above the valence band, respectively. In addition, it was found that the emission band at 1.27 eV is associated with an acceptor level located at 0.3 eV below the valence band.

Capozzi [32], in another investigation, has focused on the PL spectra of Cu doped and undoped p-type GaSe with  $\epsilon$ -structure. Doping is performed by adding the Cu atoms into the growth ampoule. It has been observed that main difference between the PL spectra of undoped and doped crystals is the appearance of two new peaks centered at 655 nm (1.892 eV) and 678 nm (1.830 eV) in the Cu doped samples at 80 K. These emission bands have been attributed to transition from donor level at about 0.195 eV below direct conduction band to acceptor level located at 31 meV and transition from the donor level to acceptor level 93 meV above valence band, respectively.

Impurity levels in Cd doped p-type GaSe samples were reported in a study performed by Shigetomi et al. in 1991 [33]. Three PL bands related to impurity levels were observed with emission energies 1.95, 1.75, and 1.62 eV at 77 K. The peak centered at 1.95 eV was attributed to transition from the conduction band to an acceptor level located at 0.18 eV above the valence band. The origin of the second emission band was stated as transition from a donor level at 0.37 eV below the conduction band to valence band and the reason of the last band was given as transitions between a donor level at 0.37 eV below the conduction band and another acceptor level at 0.13 eV above the valence band. In addition, an increase in PL intensities was observed with increasing Cd concentration.

In 1999, Shigetomi et al. [34] studied PL properties of Li doped p-type GaSe samples. At 77 K, it was observed that a new emission band centered at 2.03 eV

appeared and grew as GaSe samples doped with Li and as the doping concentration increased. The recombination associated with this emission band was considered as transitions from the conduction band or shallow donor levels to acceptor level at 0.08 eV.

Abdinov et al. [44] have carried out an investigation about the effects of PL from GaSe and InSe single crystals doped with rare-earth dopants (Gd, Ho, and Dy). The result of this study is that PL properties of rare-earth-doped GaSe and InSe single crystals are independent from the nature of the dopant. Moreover, it has been found that PL spectra of both materials depend on the doping level.

PL measurements have been made on Te doped p-type GaSe crystals by Shigetomi et al. [37] and the PL spectrum of the Te doped sample have been compared with the results of the Se excess sample and stoichiometric GaSe crystal at 77 K. For stoichiometric sample two emission peaks attributed to direct free exciton and direct bound exciton to acceptor levels have been observed at 2.098 and 2.078 eV, respectively. For Se excess sample, a PL band has appeared at 2.036 eV in addition to direct free exciton band at 2.098 eV. It is reported that the peak at 2.036 eV is due to the one phonon replica of indirect free exciton. In PL spectra of Te doped sample it has been observed that another emission band centered at 1.73 eV forms and the intensity of the line at 2.036 eV is increased. It has been stated that this new line is due to transition from conduction band to acceptor level at located 0.44 eV above the valence band. Appearance of the peak at 1.73 eV and an increase in the intensity of the line at 2.036 eV is attributed to increase in the lattice disorders and defects by doping Te atoms in to the GaSe samples.

In 2005, Shigetomi et al. [38] studied the recombination mechanisms in layered p-type GaSe semiconductor doped with As, Bi, and Sb. The PL properties coming from impurity levels caused by the dopants atoms are dominated by a broad line at about 1.7 eV. Using the results of the temperature dependence of emission band energy and intensity and the excitation intensity dependence of peak energy, it was found that this line results from transitions between shallow donor located at about 0.08 eV below the conduction band and the deep acceptor level at about 0.6 eV above the

valence band.

Radiative transitions related to Ag atoms doped into GaSe crystals have been investigated by Shigetomi et al [39]. It was reported that emission spectra are dominated by two bands at 2.02 and 1.74 eV. These lines were attributed transitions from the conduction band to the acceptor level at 0.07 eV above the valence band and the donor level at 0.31 eV below the conduction band to the same acceptor level, respectively. Moreover, it was observed that the intensities of lines increase with increasing Ag concentration.

The effect of annealing on PL spectra of GaSe samples have been a subject of another study performed by Shigetomi et al. [45]. It has been reported that PL spectra of as grown GaSe samples contain two emission bands centred at 2.10 and 2.03 eV at 77 K and they are due to recombination of direct free exciton and indirect free exciton, respectively. Annealing processes performed at 600, 700, and 800 °C, have showed that although the PL intensity of the line at 2.10 eV decreases with increasing annealing temperature, the peak energy remains constant. In addition, a new band with maximum at 1.45 eV has been observed with annealing and the intensity of this band has enhanced with increasing annealing temperature. The origin of the band is attributed to vacancy- acceptor complex. Moreover, it has been reported that the peak appeared in the spectra of annealed samples may be due to the acceptor level at 0.45 eV above the valence band.

In 1998, Shigetomi et al. [40] focused on the radiative recombination mechanisms in P-doped p-type GaSe single crystals. It was observed that PL spectra of doped samples are dominated by the emission band centered at 1.355 eV. The reason of this PL peak was stated as recombination associated with the acceptor level located at 0.45 eV.

The energy levels related to Cr, Mn atoms in  $\epsilon$ -GaSe single crystals have been studied by Chung et al. [35]. It has been reported that PL spectrum of 0.05 % mole Cr doped samples contains an emission band at 1.942 eV in addition to excitonic bands. As the doping level has increased, this line has grown and two more lines at

1.876 and 1.787 eV have appeared. PL measurements with Mn doped samples at 12 K have showed that a wide band centered at 1.804 eV appears and grow as Mn doping concentration increases. In addition, in this spectrum direct and indirect free and bound excitons have been observed.

Previous studies concerning PL properties of GaSe single crystals showed that although there were solubility and segregation problems in the chemically doping method, many studies have been performed about PL features of chemically doped GaSe. However, although ion implantation technique does not include such problems, only one study existed in the literature by Capozzi et al. [46] which gave the effects of implantation on PL properties of GaSe. In his study, Cu implantation has been performed.

### **1.2.2 Previous Studies about PL Properties of InSe**

The first studies about the luminescence features of InSe single crystals have demonstrated the presence of a wide band with a maximum at 1100 nm at temperature 77 K. Moreover, a decrease in the intensity of this band has been observed with increasing temperature [47]. Another earlier investigation was performed by Kurbatov et al. in 1971 [48]. It was reported that the PL spectra of InSe single crystals are strongly affected by deformation of the sample. The spectrum obtained from undeformed regions at 90 K showed that the emission spectrum contained only a band located at 1.325 eV and there was no band in the region of 1100 nm. This line centered at 1.325 eV was attributed to recombination of free exciton.

Photoluminescence of n-type InSe single crystals grown by Bridgman method also have been studied by another group [49] in 1974. The reason of the difference of the results reported in [47] and [48] were interpreted as probably the difference between the excitation densities [49]. This study was focused on the dependence of PL spectra for three different samples on temperature. Measurements showed that emission spectrum changes sample to sample. Moreover, it was found that below 60 K the

spectrum has the line located at 936 nm and a broad long wavelength band consisting of at least two overlapping bands. However, the origin of the long wavelength band was not explained.

In 1986, Kazuaki et al. [50] studied influence of defects on PL behaviour of InSe layered crystals. In the experiments three samples containing different defect concentration were used. In the spectrum of InSe sample with low defect concentration (a nearly perfect crystal) at 14 K it was observed three emission bands with excitonic origin. They located at 1.333, 1.334, 1.336 eV. It was reported that the spectrum of the sample containing stacking faults consisted of a new broad peak at 1.328 eV and two lines centered at 1.333 and 1.336 eV. In addition, measurements repeated for a sample with mechanical damage introduced in cleaving process and another peak at 3.14 eV was observed. The conclusion of this study was that the intensity of the broad structures below 1.330 eV was enhanced with increasing lattice disorder.

Low temperature PL properties of n-type InSe layered semiconductor crystals have been performed by Abay et al. [51]. Four emission bands located at 1.334, 1.306, 1.288, and 1.232 eV have been observed at 10 K. The first line has been attributed to recombination of direct free exciton because it is same as that reported in ref [16]. It has been stated that the origin of the second peak is transition from impurity level at 43 meV below the conduction band to valence band. The reason of the emission band at 1.288 eV has been reported as recombination of donor acceptor pair. Because it has been known that a donor state at 43 meV exists and the band is 61 meV lower than the band gap, this band has been attributed to transition between the donor level at 43 meV below the conduction band to acceptor level located at 18 meV above the valence band. In addition, the broad band at about 1.232 eV has been assigned to transition within an impurity vacancy-complex.

The dependence of PL properties of InSe single crystals on impurity atoms also has been investigated. In order to observe effects of dopant atoms InSe single crystals chemically doped with Hg [53], Ge [54], Sn [55], As [55], Sb [56], Si [57] and Cd [58], implanted with Sn [59].

PL features of p-type InSe layered crystals doped with Cd atoms have been studied by Shigetomi et al [58]. The study has been based on a comparison of PL spectra of undoped and doped InSe samples with Cd in the range 0.1 to 5 at. %. It has been reported that at 77 K PL spectrum of undoped sample contained only one PL band attributed to recombination of free exciton with a maximum at 1.33 eV while in the spectra of Cd doped samples a new broad peak located at 1.21 eV has been observed. Moreover, the intensity of the peak observed in doped samples enhanced with increasing dopant concentration. It has been found that this band was not due to impurity-band transitions because the sum of the activation energy of the band and the peak energy was larger than the band gap energy of InSe.

In 1998, PL measurements were made on undoped and Hg doped p-type InSe single crystals by Shigetomi et al. [53]. In the spectrum of undoped and doped samples, the emission band at 1.327 eV has been observed and it was supposed that this line was due to recombination of bound exciton. In addition, the spectra of InSe samples doped with Hg contain an extra band centered at 1.237 eV. Using the temperature dependence of its intensity, it was found that the activation energy is about 0.07 eV. Because the sum of the 1.237 eV emission peak and the activation energy is smaller than the band gap of InSe at 77 K, it was stated that this peak was not considered to be an impurity band transition. Moreover, in this study a donor level at 0.036 eV below the conduction band was found by electrical measurements. Therefore, the peak located at 1.237 eV was attributed to transition from this donor level to the acceptor level at 0.07 eV.

Shigetomi et al. studied the impurity levels in Sn doped p-type and As doped n-type InSe crystals [55]. Also, PL spectrum of undoped sample has been measured. In all samples' PL spectra, at 77 K an emission band at 1.327 eV, which was 16 meV lower than the band gap energy, has been observed. Because the ionization energy of the ground state for  $n=1$  exciton is 14 meV, this line was attributed to recombination of free exciton or recombination of bound exciton. For As doped sample any impurity band was observed on the lower energy side of the excitonic peaks. In the PL spectrum of Sn doped sample, a new emission band at 1.275 eV, which is 68 meV lower than the forbidden energy of the InSe at 77 K, was observed in addition

to the 1.327 eV band. This line was considered to be the transition from the donor level at 0.06 eV to valence band or shallow acceptor level.

Impurity levels in n-type InSe doped with Ge has been studied by Shigetomi et al. [54] in the spectra of undoped sample, one emission band at 1.327 eV has been observed. The spectra of doped samples contain two additional peaks centered at 1.28 and 1.25 eV. It has been reported that the origin of the peak observed all spectra was recombination of free exciton. Using the result of electrical and optical measurements, it has been found that two emission bands at 1.28 and 1.25 eV were associated with the donor levels located at 0.06 and 0.09 eV below the conduction band.

Gridin et al. [59] in 1992 focused on the temperature dependent PL properties of Sn implanted InSe single crystals. Two broad emission bands centered at about 2.2 and 1.8 eV were observed in the spectra of implanted sample measured at 5 and 263 K. In addition, it was reported that the peak with higher energy has a positive shift with the decrease of temperature, while other line has a negative shift. This behaviour was not observed for unimplanted samples in which energies of peaks increased with decreasing temperature. It was stated this shift was probably due to the introduction of deep impurity levels with implantation.

The studies mentioned about PL of InSe layered single crystals show that there are many studies about the photoluminescence features of chemically doped InSe single crystals. However, the study in which Sn implantation has been performed by V. V. Gridin et al. [59] is the only article dealing with the PL of implanted InSe. Moreover, in the literature there is no study about the emission properties of annealed InSe crystals.

Tables 1.3. and 1.4. give a review of the PL peaks for the crystals GaSe and InSe, respectively.

Table 1.3. Ten of the previously observed peaks in the PL spectra of GaSe

ref.	dopant	Temp. (K)	line1	line2	line3	line4	line5	line6	line7	line8	line9	line10
25		4.2 K	583.25494nm (2.1260eV)	583.94161nm (2.1235eV)	587.39934nm (2.1110eV)	589.07363nm (2.1050eV)	589.4937nm (2.1035eV)	590.33563nm (2.1005eV)	591.03908nm (2.0980eV)	592.1681nm (2.0940eV)	592.73423nm (2.0920eV)	593.15953nm (2.0905eV)
		77K	584.62989nm (2.121eV)	587.95638nm (2.1090eV)	588.65417nm (2.1065eV)	589.07363nm (2.1050eV)	589.91437nm (2.1020eV)	590.33563nm (2.1005eV)	591.03908nm (2.0980eV)	596.15385nm (2.080eV)	599.03382nm (2.070eV)	607.2478nm (2.042eV)
26		4.2K	607.843nm (2.04eV)									
			591.885nm (2.095eV)	593.870nm (2.088eV)								
			588.235nm (2.108eV)									
27		77K	591.039nm (2.098eV)	599.323nm (2.069eV)	608.141nm (2.039eV)							
24		80K	591nm (2.098eV)	597.6nm (2.0751eV)	609.2nm (2.0354eV)	620.3nm (1.9982eV)						
		room	639.8nm (1.938eV)	621.3nm (1.996eV)								
28		80K	586.8nm (2.113eV)	591.0nm (2.098eV)	596.8nm (2.078eV)	609.3nm (2.035eV)	619.4nm (2.002eV)					
			591nm (2.098eV)	597.6nm (2.075eV)	609.2nm (2.035eV)	620.3nm (1.999eV)	644.8nm (1.923eV)	662.2nm (1.872eV)	700.3nm (1.771eV)	741.8nm (1.672eV)		
32		80K	591nm (2.098eV)	597.6nm (2.075eV)	609.2nm (2.035eV)	620.3nm (1.999eV)	644.8nm (1.923eV)	655.2nm (1.892eV)	662.2nm (1.872eV)	677.5nm (1.830eV)	700.1nm (1.771eV)	741.7nm (1.672eV)
	Cu	80K	591nm (2.098eV)	597.6nm (2.075eV)	609.2nm (2.035eV)	620.3nm (1.999eV)	644.8nm (1.923eV)	655.2nm (1.892eV)	662.2nm (1.872eV)	677.5nm (1.830eV)	700.1nm (1.771eV)	741.7nm (1.672eV)
29		80K	591nm (2.098eV)	596.728nm (2.078eV)	609.337nm (2.035eV)	619.38nm (2.002eV)	659.575nm (1.88eV)	751.515nm (1.65eV)				
31		77K	590.476nm (2.10eV)	610.837nm (2.03eV)								
	Zn	77K	590.476nm (2.10eV)	610.837nm (2.03eV)	708.571nm (1.75eV)	760.736nm (1.63eV)	976.378nm (1.27eV)					
33		77K	590.476nm (2.10eV)	610.837nm (2.03eV)								
	Cd	77K	590.476nm (2.10eV)	610.837nm (2.03eV)	635.897nm (1.95eV)	708.571nm (1.75eV)	765.432nm (1.62eV)					
34		77K	591nm (2.098eV)	609nm (2.036eV)								
			591nm (2.098eV)	609nm (2.036eV)	610.837nm (2.030eV)							
60		77K	590.476nm (2.10eV)	610.837nm (2.03eV)								
	Mn	77K	590.476nm (2.10eV)	610.837nm (2.03eV)	623.115nm (1.99eV)	681.32nm (1.82eV)	898.551nm (1.38eV)					
30		10K	644nm (1.925eV)	695nm (1.784eV)								
44		77K	~590nm (2.10eV)	~600nm (2.067eV)	610nm (2.033eV)							
			~600nm (2.067eV)	~800nm (1.55eV)	~1050nm (1.181eV)							
	Dy	77K	586nm (2.116eV)	613nm (2.023eV)	791.8nm (1.566eV)	792.2nm (1.565eV)	794.4nm (1.561eV)	794.9nm (1.560eV)	797.2nm (1.555eV)	800.1nm (1.550eV)	802.8nm (1.454eV)	804.0nm (1.542eV)
36		10K	591nm (2.098eV)	596.73nm (2.078eV)								
37		77K	609.04nm (2.036eV)	716.76nm (1.73eV)								
	Te	77K	590.476nm (2.10eV)	610.837nm (2.03eV)								
38		77K	746.988nm (1.66eV)									
	Sb	77K	725.146nm (1.71eV)									
61		77K	591nm (2.098eV)	~600nm (2.067eV)	611nm (2.03eV)							
			592nm (2.094eV)	604nm (2.053eV)	613nm (2.023eV)	622nm (1.993eV)	692nm (1.791eV)	908nm (1.36564eV)				
	0.05%Mn	77K	592nm (2.094eV)	660nm (1.87879eV)	742nm (1.67116eV)	758nm (1.63588eV)	908nm (1.36564eV)					
	0.1%Mn	77K	590.476nm (2.10eV)	610.837nm (2.03eV)								
39		77K	590.476nm (2.10eV)	610.837nm (2.03eV)	613.861nm (2.02eV)	712.644nm (1.74eV)						
			589.634nm (2.103eV)	671.178nm (2.084eV)	601.65nm (2.061eV)	604.583nm (2.051eV)	614.165nm (2.019eV)					
	0.05%Mn	12K	589.634nm (2.103eV)	671.178nm (2.084eV)	601.65nm (2.061eV)	604.583nm (2.051eV)	614.165nm (2.019eV)	687.361nm (1.804eV)				
	1%Mn	12K	687.361nm (1.804eV)									
		12K	589.634nm (2.103eV)	603.994nm (2.053eV)	611.44nm (2.028eV)	619.071nm (2.003eV)						
	1%Cr	12K	638.52nm (1.942eV)	660.981nm (1.876eV)	693.9nm (1.787eV)							
40		77K	590.476nm (2.10eV)	610.837nm (2.03eV)								
			590.476nm (2.10eV)	610.837nm (2.03eV)	915.13nm (1.355eV)							
	P	77K	590.476nm (2.10eV)	610.837nm (2.03eV)								

Table 1.4. Previously observed PL bands in InSe single crystals

reference	dopant	Temp. (K)	line1	line2	line3	line4	line5
49		4.2K	930.23nm (1.333eV)	938.68nm (1.321eV)			
		4.2K	944.4nm (1.313eV)				
		4.2K	942.25nm (1.316eV)				
62		14K	928.14nm (1.336eV)	929.53nm (1.334eV)	930.23nm (1.333eV)		
		14K	928.14nm (1.336eV)	929.53nm (1.334eV)	930.23nm (1.333eV)	933.73nm (1.328eV)	
		14K	928.14nm (1.336eV)	929.53nm (1.334eV)	930.23nm (1.333eV)	933.73nm (1.328eV)	943.68nm (1.314eV)
48		90K	935.85nm (1.325eV)				
63		5.2K	928.14nm (1.336eV)	929.19nm (1.3345eV)	930.23nm (1.333eV)		
59		5K	563.64nm (2.2eV)	688.89nm (1.8eV)			
47	Sn	77K	1100nm (1.127eV)				
51		10K	929.53nm (1.334eV)	946.46eV (1.306eV)	962.73nm (1.288eV)	1006.5nm (1.232eV)	
53	Hg	77K	936.555nm (1.327eV)	1002.42nm (1.237eV)			
54		77K	936.555nm (1.327eV)				
	0.05at%Ge	77K	936.555nm (1.327eV)	968.75nm (1.28eV)			
	0.5at%Ge	77K	936.555nm (1.327eV)	968.75nm (1.28eV)	992nm (1.25eV)		
55		77K	936.555nm (1.327eV)				
	Sn	77K	936.555nm (1.327eV)				
	As	77K	936.555nm (1.327eV)	972.55nm (1.275eV)			
58		77K	932.33nm (1.33eV)				
	Cd	77K	932.33nm (1.33eV)	1023.1nm (1.212eV)			

### 1.3 Present Study

In this work, PL properties of GaSe and InSe single crystals grown by Bridgman-Stockbarger technique in the Crystal Growth Laboratory of Physics Department at METU were investigated by photoluminescence spectroscopy. In order to examine the effect of Ge-implantation on temperature dependent emission spectra of the layered crystals, the samples were implanted by Ge ions with 100 keV energy and  $1 \times 10^{13}$ ,  $1 \times 10^{14}$ , and  $1 \times 10^{15}$  ions/cm<sup>2</sup> doses at room temperature. In addition, annealing was performed for some GaSe and InSe samples at 500 °C for 30 minutes in order to analyse their photoluminescence spectra and compare them with unannealed samples.

The outline of this thesis is given as follows: chapter 2 presents a detailed theoretical background for crystal growth, ion implantation and photoluminescence spectroscopy. In chapter 3 experimental techniques, including the crystal growth procedure, starting from crucible cleaning, synthesis to sample preparation for measurements, ion implantation and annealing processes and photoluminescence measurements, are explained. Moreover, in this chapter, experimental set ups for all used techniques are summarized. In chapter 4, photoluminescence results are given with discussions. Finally, the conclusions are presented in the last chapter.

## **CHAPTER II**

### **THEORETICAL CONSIDERATIONS**

#### **2.1 Introduction**

In this chapter, commonly used crystal growth techniques, ion implantation and annealing processes are summarized. A detailed theoretical background for photoluminescence spectroscopy and related mechanisms resulting in light emission are given.

#### **2.2 Crystal Growth**

In order to fabricate many solid state devices such as modern integrated circuits, single crystal semiconductor substrates are required. However, single crystals are rarely found in nature. Most crystalline materials exist in polycrystalline forms, made up of a number of small variously-oriented crystal regions, often referred to as grains, separated from each other with their grain boundaries. Therefore, the preparation of single crystal semiconducting materials gains importance for the improvement of solid state device technology [3, 64].

The requirements of the controlled conditions in laboratories make the production of single crystals difficult. However, with the increasing technological advancements improved special conditions can be obtained for many scientific studies and technical applications single crystals can be produced. The growth of single crystal can be

mainly divided into two categories [3]. First category is the epitaxial growth techniques to grow layers on a substrate material. Such crystals are used to produce electronic devices. In these techniques, the substrate material acts as a seed crystal and a crystalline material grows onto it. The grown single crystal film has the same orientation and the same structure with the substrate crystal. If epitaxially grown material is the same material with the substrate the method is called homo-epitaxy and if a different material is grown then the process is called hetero-epitaxy. Chemical Vapour Deposition (CVD), Molecular Beam Epitaxy (MBE), Liquid Phase Epitaxy (LPE) and Solid Phase Epitaxy (SPE) are methods used to grow epitaxial single crystal films [65]. The second category is the growth of bulk crystals. Most substrates used in many electronic applications are fabricated from bulk crystals. The crystallization of bulk single crystals can be produced using three distinct ways [66]:

1. *The growth from solid to solid:* It is a solid-solid process containing solid to solid phase transitions. These processes are used to produce certain metals and in certain cases where a structural change of a crystal occurs between the melting point and the room temperature.
2. *The growth from melt to solid:* It is a liquid to solid process involving liquid to solid phase transitions. It is a widely used technique for the production of single crystals and there are many methods in which the liquid to solid phase transition occurs. In this process single crystals are grown from a melt by lowering the temperature below the freezing point of the melt.
3. *The growth from vapour to solid:* It is a vapour-solid process involving vapour to solid phase transitions. These processes include sublimation which is the direct change from gas to solid without passing from liquid state by application of an appropriate temperature gradient. Another process is the vapour phase reactions in which the vapour is transported in the growing area and crystal grows as a product precipitated from the vapour phase as a result of a chemical reaction between vapour species at the surface.

As it is mentioned before, crystallization from melt is most commonly used process. It is achieved by placing a molten material in a temperature gradient and then cooling the liquid below its freezing point so that it solidifies gradually from one end to the other end. In another words, an ingot is progressively frozen from the cold end to the hot end with the help of a temperature gradient. One of the widely used methods to grow single crystal from melt is Bridgman-Stockbarger technique. In this technique the melt is contained in a crucible and it is lowered through a furnace. The temperature is adjusted so that the molten material starts to solidify from the lower end of the crucible and frozen face moves slowly up to it. About 40 % of the produced single crystals are grown by using this method. Its advantages are that single crystals with good dimensional tolerances are produced, the apparatus is simple and very little operator attention is required [67]. One disadvantage of the technique stems from the crucible which can give rise to contamination of the grown crystal. Due to the fact that the crystals which were used for this experimental study have been grown by Bridgman technique, the detailed explanation of this method will be given in the next chapter.

Frequently used other techniques are Czochralski growth technique and the zone refining method. In Czochralski method single crystals are grown from the molten material by pulling. A rotating seed single crystal is lowered into a melt and the seed crystal temperature is adjusted at just below the melting point of the material. When the thermal equilibrium of the system is provided, the seed is slowly raised from the melt. The major advantage of growing the single crystal by using this technique is the possibility of production of a crystal in large diameters. Today, crystals of 30 cm in diameter and 1 m in length are commercially grown by using this growth technique. Another mostly used technique to grow a single crystal is the zone refining method. In this technique, only a part of the polycrystalline material is melted and this liquid zone is moved slowly from the seed to the poly rod, melting the poly material just above the molten material. As a result of the controlled solidification of the melt on the seed, the polycrystalline material is converted into the single crystal [68, 69]. The use of a moving molten zone provides the purification over the starting material and by repeating the process the purity of the material can be further increased. Therefore, this technique is called zone refining method [3].

### 2.3 Ion Implantation and Annealing

In order to modify the electrical and optical characteristic of semiconductors, impurities can be introduced into the crystals. This process is known as doping and can be done by two ways. One of them is chemical doping in which dopant element is directly added to the growth ampoule. However, in this method the impurity concentration is very small and solubility and segregation of the dopant agents can take place in the host material. Second method used for doping is ion implantation in which ions having high energies are sent to the crystals [64]. The main advantages of this technique can be listed as below. It is a short time process and it provides good homogeneity. It has wide dopant concentration range ( $10^{13}$ - $10^{21}$  ions/cm<sup>2</sup>) and it provides precise control on the number of implanted ions [68]. In addition, solubility and segregation of the dopant atoms in the target material is eliminated by using this method.

When the energetic ions enter the sample, they collide with the nuclei of the lattice atoms and the cloud of electrons of the atoms transferring their energy to them. If the ions collide with nuclei, this stopping mechanism of the ions is called nuclear stopping. In nuclear collisions, when the transferred energy to the lattice atom is higher than lattice binding energy, the atoms breaks and it collide with other lattice atoms while moving inside the sample and transfer enough energy to break free from the lattice binding energy. This process goes on until none of the atom has sufficient energy to make free other lattice atoms [68]. If the ions collide with electrons in the crystal, this is called electronic stopping mechanism. In these collisions, the transferred energy to the electrons causes the excitation of electrons to the higher energy levels or ejection of them from the atom (ionization). Because of these two stopping mechanisms dopant atoms lose their energy in the material and they eventually rest inside the sample [70]. The energy loss per unit distance due to nuclear and electronic stopping mechanisms has been modelled by combining the contributions of these two independent collisions by Lindhards, Schorff, and Schiott (LSS) [64]. The energy loss per unit distance is given by

$$\left(\frac{dE}{dx}\right)_{total} = \left(\frac{dE}{dx}\right)_{nuclear} + \left(\frac{dE}{dx}\right)_{electronic} \quad (2.1)$$

where the nuclear and electronic losses depend on the energy of incident ion.

The accelerated ions lose their energy through collisions and stop at some depth within the material. The total distance travelled by the ion before coming to rest is called range  $R$ , and the projection of the range along the axis of incidence is called the projection range  $R_p$  [71]. These two parameters are illustrated in Fig.2.1.

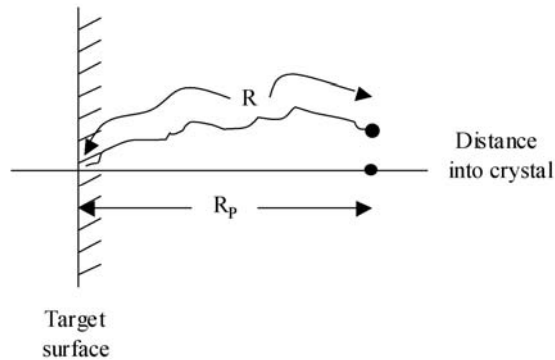


Fig.2.1. Schematic representation of the ion range  $R$  and projected range  $R_p$  [71].

As stated before, when the ions enter the material, they transfer their energy to lattice atoms due to the collisions with electrons and nuclei. Unlike the electronic collisions, with nuclear collisions sufficient energy can be transferred to the lattice so that the locations of the lattice atoms may change. This results in substitutional lattice disorder (damage) [65]. The energy, dose and mass of the ions and temperature of implantation affect the lattice disorder created by implanted ions. Fig.2.2 shows the distribution of damage produced by two ions with different masses.

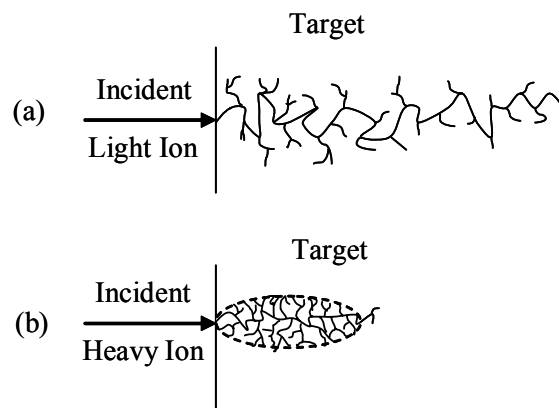


Fig.2.2. Damage resulted from (a) light ions and (b) heavy ions [64].

In ion implantation process, the number of implanted ions is so large that the self-annealing can not remove the crystal damage at the room temperature. Therefore, the material has to be annealed in order to repair the lattice damage and to put dopant atoms on substitutional sites. In this process to increase thermal vibrations of the atoms high temperature is used. With increase in thermal motion, the atoms find the substitutional positions with the lowest free energy in the crystal lattice and they stay there [64].

## **2.4 Luminescence**

The characterization of materials especially semiconductors is a broad scientific area because a comprehensive survey must be conducted in order to determine whether they can be used in many devices. This analysis depends on various experimental methods. The most effective ones are techniques in which electromagnetic radiation is used since basic properties of semiconductors can be examined with the knowledge of how they react to light. Moreover, the ability of optical analysis contributes to application areas specially optoelectronic applications of semiconductors. Therefore, they are widely used. One of the common spectroscopic techniques so as to yield information on the fundamental properties of semiconductors is luminescence spectroscopy. Luminescence means the light emission after some energy was given to the material. It was reportedly first observed in 1603 by Cascariolo [72]. He heated some natural barium sulphate with coal and saw that the cooled material glowed at night. After that, the term “luminescence” (the literal translation from Latin is “weak glow”) was introduced into the literature by a German physicist Wiedemann in 1888 [73].

There are several ways for production of luminescence depending on the cause or duration. Among them, the most commonly used method is photoluminescence, observed after the absorption of photons of energy greater than the forbidden energy of the material as a radiation of photons of energy lower than the excitation photons. Another way to produce light is to excite the sample by applying an electric current passed through it or a strong electric field, called electroluminescence. Thermoluminescence, the light emission from the sample by heating and

cathodoluminescence which can be described as excitation by the electron bombardment are also other types of luminescence [2, 74]. In addition, two forms of luminescence can be identified, depending on the light emission time: fluorescence and phosphorescence. Fluorescence refers to the release of light that lasts no more than about 10 nanoseconds after it begins while phosphorescence takes longer than 10 nanoseconds sometimes many hours or even days [1].

## 2.5 Photoluminescence Spectroscopy

Photoluminescence spectroscopy is a sensitive, non-contact and non-destructive tool, suitable to characterize point defects, such as impurities (donors, acceptors) and native or intrinsic defects in crystals. It can be also used for the determination of the band gap energy of the material [2]. In addition, using this method it is possible to have an idea about the material quality.

In photoluminescence spectroscopy, light with energy greater than the band gap of studied material are directed onto surface of the semiconductor material, this incident photon beam is partially reflected, absorbed, and transmitted by the material being probed. The absorbed photons cause excitation of electrons to the conduction band and as a result of this, electron-hole pairs are created in the semiconductor. Then, these electrons fall back to their equilibrium states. This process may include the emission of light (a radiative process) or may not (non radiative process). Photons produced as a result of the various recombinations of electrons and holes are emitted from the sample surface and it is the resulting photon emission spectrum that is studied in photoluminescence. Because there is no light emission from non-radiative recombination events, they are not detected with photoluminescence measurements. It can be possible to explain photoluminescence processes in three general parts [74]:

- 1) *Excitation*: Electrons are excited from the filled valence band to the empty conduction band by an external source of energy. As a result of this, electron hole pairs (EHPs) are created in the material.

2) *Thermalization*: The promoted electrons give up energy to the lattice of the material and cools down to the minimum of the conduction band. In another word, excited electrons above the conduction band edge falls down and reaches thermal equilibrium with the lattice.

3) *Recombination*: The electron hole pairs recombine and the electron return to their original state. As a result of this event, the excess energy is released by radiatively or non-radiatively. In this process, many recombination mechanisms can take place.

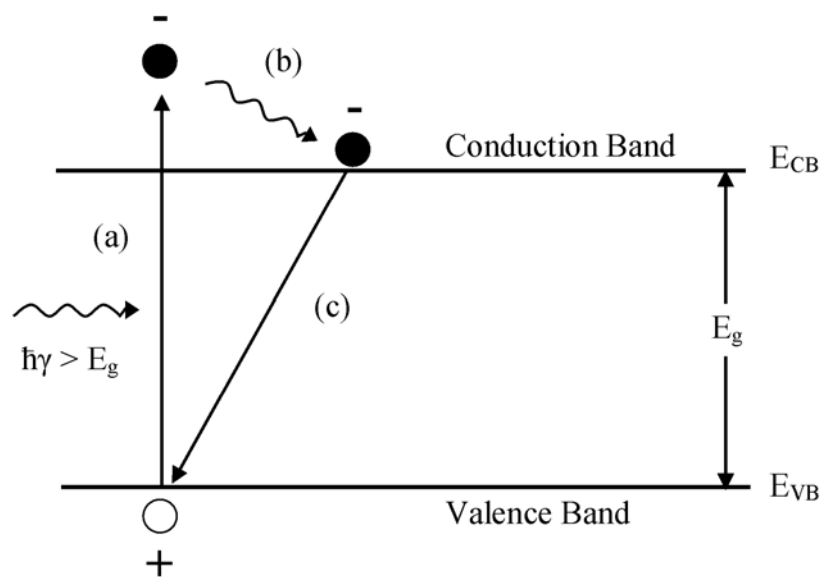


Fig.2.3. Schematic showing of photoluminescence processes [4]. (a) The creation of an electron hole pair by optical excitation. (b) Releasing energy of the promoted electron in the conduction band (c) The recombination of an electron in the conduction band and a hole in the valence band resulting in the emission of light

### 2.5.1. Recombination Processes

When electrons absorb energy greater than the band gap from external sources, they are promoted to the conduction band, creating electron hole pairs. When the electrons make transitions to the initial states (i.e., recombine with the holes), the energy is released. This return process can occur radiatively or non-radiatively. Thus, it is said to be radiative or non radiative recombination. If the electron hole pairs recombine through radiative recombination, the energy of the emitted light is related to the energy difference in levels between the two states. Therefore, using

photoluminescence spectroscopy, it is possible to obtain information about the recombination mechanisms within the material.

Electrons in the conduction band may transfer to the valance band either directly or indirectly. If conduction band and valance band do not lie at the same momentum level, this transition is said to be indirect transition and for this process to provide momentum conservation a participation of an extra particle, i.e., phonon, energy of lattice vibrations, is necessary. Even, sometimes, more than one optical phonon emission can be observed during the transition. However, for direct transitions, there is no a phonon contribution of because momentum within the lattice is conserved [3].

As it is mentioned before, because of impurities and defects in semiconductors, discrete energy levels are formed within the band gaps of the semiconductor materials. These levels act as capturing centers and they can be divided into two groups [75]: (1) Trapping centers: if the captured carrier has a greater probability of re-excitation to the free state than of recombination, this level is called trapping center. (2) Recombination center: if the most probable event of the captured carrier is recombination, this energy level is called recombination center. In addition to this classification, the energy levels in the band gap can be categorized as shallow and deep levels according to their depth from the nearest band edges. In general, deep levels behave as recombination centers because they have large capture cross-sections [2].

Recombination, a quite complicated process, can occur by several different mechanisms, all of which result in the annihilation of an electron and a hole. Fig.2.4. represents the most common radiative recombination mechanisms. In this figure  $E_c$  is the minimum energy of conduction band and  $E_v$  is the maximum energy of the valance band. In addition,  $E_D$  and  $E_A$  illustrate the energy of donor level and acceptor level, respectively. Band to band transition, free to bound transitions (donor level to valance band and conduction band to acceptor level), donor to acceptor transition, and excitonic transitions, related to free and bound excitons, are radiative transitions shown in Fig.2.4.

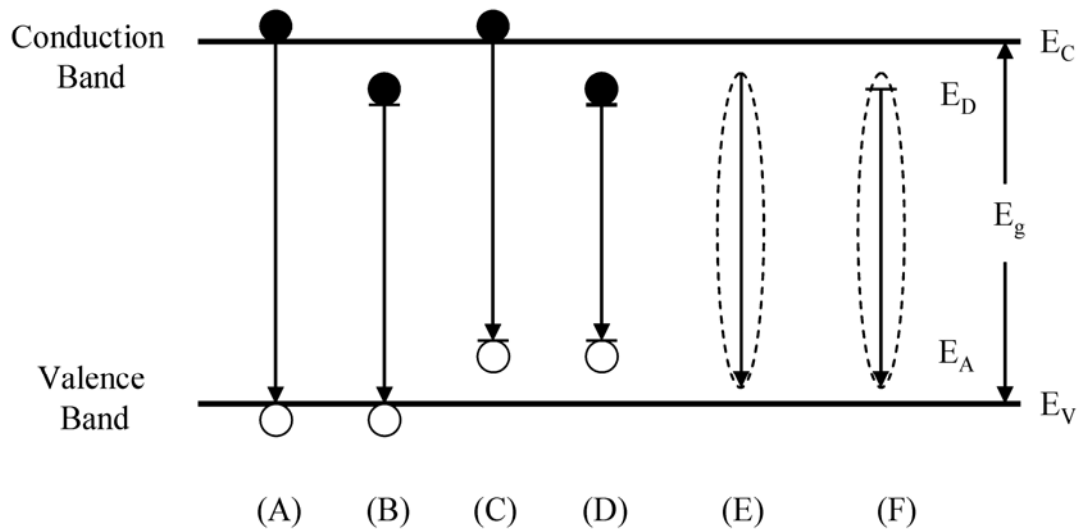


Fig.2.4. The most common radiative recombination mechanisms. (A) Band to band transition, (B) donor to valence band transition (C) conduction band to acceptor transition, (D) donor to acceptor transition, (E) free exciton recombination, and (F) bound-exciton recombination

### 2.5.1.1 Band to Band Transitions

In perfect semiconductors, during thermalization process, electrons and holes aggregate at the minimum of conduction band and the maximum of valence band, respectively. The recombination of these electrons and holes at the conduction and valence band extrema is known as band to band recombination. The schematic representation of this transition is shown in Fig.2.4(A). Since it involves free holes and free electrons, this type of recombination is sometimes called free to free recombination. For this transition, photons with energy close to the band gap energy of the materials are produced. Therefore, band to band transition can be used for the estimation of the band gap energy, the forbidden energy between valence band maxima and conduction band minima.

For direct semiconductors, recombination is observed as a transition across the minimum energy gap, from the most probably filled states at the conduction band to the states most likely to be unoccupied at maximum of the valence band by emitting the light whose energy is given by

$$\hbar\gamma = E_f - E_i \quad (2.2)$$

In this equation,  $E_f$  and  $E_i$  are the energies of final and initial states, respectively. For indirect gap semiconductors, because the transition occurs between energy levels with different momentum values, a change in both energy and momentum is required in order to complete such a process. Because the photon cannot provide a change in momentum levels between the conduction band valence bands, momentum conservation is provided by lattice vibrations. In this process, emitted light is given by the equation:

$$\hbar\gamma = E_f - E_i \pm \hbar\Omega \quad (2.3)$$

where  $\hbar\Omega$  is energy of the phonon, and the minus and plus signs correspond to phonon absorption and phonon emission, respectively [76]. In indirect semiconductors, owing to the requirement of a phonon in order to provide momentum conservation, the probability of such a transition is significantly lower as compared with direct transitions. Representative figures of these transitions are shown in Fig.2.5.

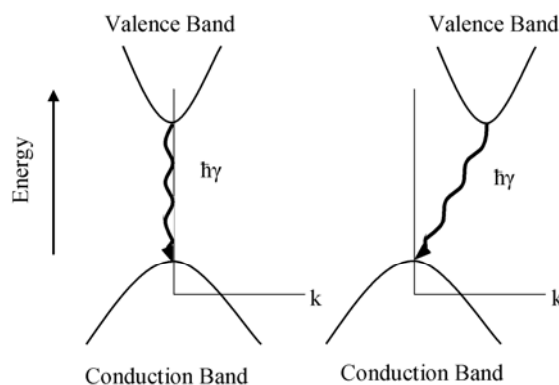


Fig.2.5. Schematic representation of radiative band to band recombination for a direct edge (a) and indirect edge (b) in energy-momentum space [77]

### 2.5.1.2 Free to Bound Transitions

Electrons and holes on impurity levels contribute the radiative transitions at sufficiently low temperatures because the thermal energy of the carriers is smaller than their ionization energy. These recombination processes can start or finish on localized states of impurities (e.g. donors and acceptors) in the forbidden energy gap. If an electron captured by a donor recombines with a free hole in the valence band, it is called the donor to valence transition (Fig.2.4(B)). In addition, conduction to acceptor transition is defined as the recombination of a free electron in the conduction band with a hole captured by an acceptor can be observed (Fig.2.4(C)). These two transitions are known as free to band transitions or band to impurity transitions. The energy of such transitions is much smaller than that of the band to band transition. The energy of photon given off is

$$\hbar\gamma = E_g - E_D \quad (2.4)$$

where  $E_g$  is the band gap of the sample,  $E_D$  is the binding energy of electrons to the donor levels. For conduction to acceptor transition the equation can be written with the holes binding energy to the acceptor levels,  $E_A$  [74].

### 2.5.1.3 Donor- Acceptor Pair Transitions

In general, semiconductors contain both donors and acceptors. In such materials, some of the electrons from donor levels can be captured by the acceptors. When an electron in the conduction band and a hole in the valence band are trapped at ionized donor  $D^+$  and acceptor  $A^-$  sites, they produce neutral donors  $D^0$  and acceptors  $A^0$ , respectively. The recombination of an electron on the neutral donor and a hole on the neutral acceptor is called donor-acceptor pair transition (DAP) (Fig.2.4(D)). This process can be represented by the reaction



The energy of photon emitted from such a transition can be given by the equation:

$$\hbar\gamma = E_g - E_A - E_D \quad (2.6)$$

where  $E_g$  is the band gap energy,  $E_A$  and  $E_D$  are the binding energy of electrons and holes to donor and acceptor levels, respectively. However, between the donors and acceptors there is the coulomb interaction. In equation 2.6 this interaction is neglected. The coulombic interaction between the carriers results in a modification of their binding energies in such a way that the donor- acceptor recombination emission is distance dependent. As a result of the contribution of the coulombic interaction, eqn. (2.6) becomes

$$\hbar\gamma = E_g - E_A - E_D - q^2 / \epsilon r \quad (2.7)$$

In this equation, the last term is the coulombic interaction between ionized donors and acceptors separated by  $r$  [78].

#### 2.5.1.4 Excitonic Transitions

**Free Excitons:** At low temperatures, coulomb attraction between a free hole and a free electron leads to the formation of an excited state in which the electron and the hole bound to each and in this state the electron can orbit about the hole as in the hydrogen atom. This form is known as exciton. When the exciton is not captured by an impurity or defect, it is called a free exciton. The excitonic energy levels are at just below the conduction band so they are typically observed at low temperatures at which  $k_B T$  is smaller than the excitonic binding energy. The recombination of these carriers is known as a free exciton recombination (Fig.2.4(E)) [79]. Because exciton is a form like hydrogen atom, the binding energy of the exciton is given by

$$E_x = -\frac{E_x^{(1)}}{n^2} \quad n=1, 2, 3, \dots \quad (2.8)$$

where,  $E_x^{(1)}$  is the ground state of the exciton,  $13.6 \times (m_r/m_0) \kappa^{-2}$  eV,  $\kappa$  is the dielectric

constant and  $n$  is an integer indicating the various allowed states of the free exciton (Fig.2.6) [1]. The ground state of the free exciton corresponds to  $n = 1$ ,  $n = 2$  corresponds to the first excited state of the free exciton, and  $n = 3$  to the second excited state, and so on. Therefore, the energy of emitted light as a result of recombination is given by eqn. (2.9) [2]:

$$\hbar\gamma = E_g - E_X \quad (2.9)$$

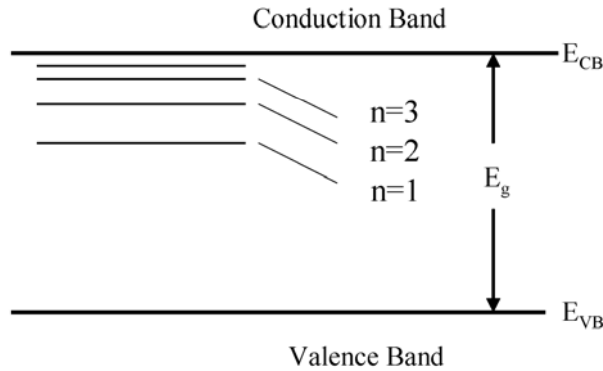


Fig.2.6. Schematic representation of the energy levels of an exciton in a semiconductor [2]

**Bound Excitons:** In a real material, many kinds of impurities or defects in neutral and ionized donor and acceptor levels exist. Free excitons in excitonic energy levels are attracted to these impurities and defects via Van der Waals interaction [78]. As a result of this, bound excitons form. The energy of the emitted photon which is the result of a bound annihilation is given by the following equation:

$$\hbar\gamma = E_g - E_X - E_B \quad (2.10)$$

where  $E_B$  is the binding energy of the exciton to an impurity or a defect level. For example, if exciton is bound to donor level (Fig.2.4(F)), then  $E_B$  will be the binding energy of the donor level.

Bound excitons can form as a consequence of trapping of free excitons by neutral and ionized donors and acceptors. Commonly observed types of bound excitons are excitons bound to neutral acceptors forming the complex  $(A^0, X)$  and excitons

bound to neutral donors denoted by  $(D^0, X)$ . In addition to these, excitons can bond to ionized donors and ionized acceptors which are symbolized by  $(D^+, X)$  and  $(A^-, X)$ , respectively. The  $(D^+, X)$  complex consists of a donor ion, an electron and a hole. The  $(D^0, X)$  bound exciton consists of a donor ion, two electrons, and a hole. The  $(A^0, X)$  complex consists of an acceptor ion, an electron, and two holes and finally excitons bound to ionized acceptor,  $(A^-, X)$ , consists of an acceptor ion, an electron, and a hole [77]. Because most semiconductor materials contain impurities and/or defects by which free excitons can be captured, the determination of the bound exciton states provides an important characterization of impurities.

## **2.6 Effects of Variations in Laser Power and Temperature on Photoluminescence Intensity**

Using the variation of photoluminescence intensity with changing the power of excitation light source it is possible to obtain information about which recombination processes have been taken place. As a result of the conducted studies from [80-82], it has been found that the photoluminescence intensity  $I$  of the near band edge photoluminescence emission lines is proportional to  $L^k$  which can be expressed as:

$$I \propto L^k \tag{2.11}$$

where  $L$  is the excitation laser intensity and  $k$  is a dimensionless exponent. For an excitation laser photon with an energy exceeding the band gap energy  $E_g$ , the coefficient  $k$  has a value between 1 and 2 ( $1 < k < 2$ ) for free and bound excitonic emissions.  $k$  value is less than 1 ( $k < 1$ ) for free to bound and donor acceptor pair recombinations [82].

Before we mention about the temperature dependence of photoluminescence intensity, variation of the energy band gap of the material with temperature will be given. The relationship between temperature and the forbidden energy of a semiconductor can be found as a result of the theoretical studies of Varshni [83]. The expression is given by

$$E_g(T) = E_g(0) - \frac{\alpha T^2}{T + \beta} \quad (2.12)$$

where  $E_g(0)$  is the value of the band gap energy which may be direct or indirect at 0 K.  $\alpha$  and  $\beta$  are constants. This equation represents satisfactorily experimental data for many semiconductors.

The variation of the band gap is believed to result from two reasons. The first one is the temperature dependent expansion of crystal lattice. As a result of theoretical treatments, it has been shown that the effect of this is linear at high temperatures while nonlinear effect has been found at low temperatures. The second reason of variation of band gap energy with temperature is electron-phonon interaction. This interaction gives rise to a decrease in  $E_g(T)$  as temperature increases because as  $T$  becomes high the second term behaves as  $-\alpha T$ , causing a decrease in  $E_g(T)$  with respect to its value at 0 K [83].

Photoluminescence intensity also changes with temperature. This variation can be used to find energy levels inside the energy band gap of the semiconductor. In order to achieve this aim, it is necessary to express the variation of photoluminescence intensity with temperature. The relation for the temperature dependence of emission intensity is given by the following equation

$$I(T) = \frac{I(0)}{1 + A \exp\left(\frac{-E_a}{k_B T}\right)} \quad (2.13)$$

where  $E_a$  is activation energy of the transition,  $k_B$  is Boltzmann's constant,  $I(T)$  is the photoluminescence intensity at temperature  $T$ ,  $I(0)$  is the photoluminescence intensity at absolute zero temperature, and  $A$  is a temperature independent constant [63, 84]. At sufficiently high temperature condition of  $A \exp(-E_a/k_B T) \gg 1$  satisfy and equation 2.13 can be written as [28, 32]

$$I(T) \propto \exp\left(\frac{E_a}{k_B T}\right) \quad (2.14)$$

This equation tells us that using the slope of the semi log plot of the photoluminescence peak intensity as a function of  $1/k_B T$ , the value of activation energy,  $E_a$ , for the transition which results in the emission can be found. Also, it is possible to calculate activation energy multiplying the slope of the semi log plot of the line intensity as a function of  $1/T$  with Boltzmann's constant.

## 2.7. Recombination Rate and Carrier Lifetime

In a semiconductor at thermal equilibrium, electrons are thermally excited from the valence band to the conduction band and then they fall into the states in the valence band again. This continuous process does not result in any change in the electron and hole concentrations with time [5].

The rate of the recombination,  $R_0$ , in thermal equilibrium is proportional to the concentration of occupied states in the conduction band (i.e., electrons) and the concentration of empty states in the valence band (i.e., holes). This may be written in the following form

$$R_0 = B n_0 p_0 \quad (2.15)$$

where  $B$  is a constant and  $n_0$  and  $p_0$  are the concentration of electrons and holes at thermal equilibrium. It is known that a semiconductor is considered to be in an equilibrium state if the equation  $n_0 p_0 = n_i^2$  is satisfied [2]. Thus, the recombination rate under thermal equilibrium is

$$R_0 = B n_0 p_0 = B n_i^2 \quad (2.16)$$

where  $n_i$  is intrinsic carrier concentration. (Because for an intrinsic semiconductor the concentration of holes and electrons are equal to each other, as intrinsic

carrier concentration the parameter  $n_i$  which refers to either electron or hole concentrations if an intrinsic semiconductor is used.)

When photons energies higher than semiconductor's band gap energy are incident on a semiconductor, as it is stated before, electrons are excited into the conduction band and electrons in the conduction band and holes in the valence band are created. These electrons and holes are called excess carriers [5]. In this case, concentrations of electrons in the conduction and holes in the valence band are higher as compared with their equilibrium values and can be given by

$$n(t) = n_0 + \Delta n(t) \quad \text{and} \quad p(t) = p_0 + \Delta p(t) \quad (2.17)$$

where  $n_0$  and  $p_0$  are thermal equilibrium concentration of electrons and holes, and  $\Delta n(t)$  and  $\Delta p(t)$  are the excess electron and hole concentrations [5]. If we look at the change in electron concentration with time, it can be written as:

$$\frac{dn(t)}{dt} = B [n_i^2 - n(t) p(t)] \quad (2.18)$$

where  $n(t) = n_0 + \Delta n(t)$  and  $p(t) = p_0 + \Delta p(t)$ . Because excess carriers are created and recombine as electron hole pairs, their concentrations are equal to each other, i.e.,  $\Delta n(t) = \Delta p(t)$ . Thus, eqn. (2.18) becomes

$$\frac{d\Delta n(t)}{dt} = -B [(n_0 + p_0) \Delta n(t) + \Delta n^2(t)] \quad (2.19)$$

Eqn. (2.19) can be simplified in a case excess carrier concentrations are small. In this case the  $\Delta n^2(t)$  term can be neglected. Moreover, if p-type material is considered ( $p_0 \gg n_0$ ), it can be written as

$$\frac{d\Delta n(t)}{dt} = -B p_0 \Delta n(t) \quad (2.20)$$

The solution to eqn. (2.20) decays exponentially from the initial excess concentration,  $\Delta n(0)$ ,

$$\Delta n(t) = \Delta n(0) \exp(-Bp_0 t) \quad (2.21)$$

Eqn. (2.21) can be written in terms of carrier lifetime, which is the average time that carriers exist between generation and recombination processes [87]. It is given for p-type material by  $\tau_n = (Bp_0)^{-1}$ . If it is substituted into eqn. (2.21), eqn. (2.22)

$$\Delta n(t) = \Delta n(0) \exp\left(-\frac{t}{\tau_n}\right) \quad (2.22)$$

is obtained [3]. In the presence of excess carriers the recombination rate is given by

$$R = R_0 + \Delta R \quad (2.23)$$

where  $R_0$  is the recombination rate of the carriers in thermal equilibrium and  $\Delta R$  is the recombination rate of excess carriers. Because recombination rate is a positive quantity, the excess carriers' recombination rate can be written using eqn. 2.23 [5]

$$\Delta R = \frac{-d(\Delta n(t))}{dt} = Bp_0 \Delta n(t) = \frac{\Delta n(t)}{\tau_n} \quad (2.24)$$

As it is understood in the above equation, the recombination rate of excess carriers in a p-type material is given in terms of excess minority carriers (electrons); therefore,  $\tau_n$  is also called minority carrier lifetime [3]. Also eqn. 2.24 says us  $R$  is proportional to  $1/\tau$  [2].

For each recombination mechanism it is possible to consider a characteristic recombination lifetime  $\tau_i$ . As it is mentioned before, recombination may occur radiatively or non-radiatively. Therefore, also, nonradiative recombination lifetimes ( $\tau_{nr}$ ) and radiative recombination lifetimes ( $\tau_r$ ) can be defined. Then, because various radiative and non-radiative recombination mechanisms occur simultaneously, the

effective lifetime  $\tau_{eff}$  can be written in the following form [87]

$$\frac{1}{\tau_{eff}} = \sum_i \frac{1}{\tau_i} = \frac{1}{\tau_r} + \frac{1}{\tau_{nr}} \quad . \quad (2.25)$$

In addition, it is possible to define the radiative recombination efficiency  $\eta$ , which is the ratio of the radiative recombination rate  $R_r$  to the total recombination rate  $R$ . It is given by

$$\eta = \frac{\tau}{\tau_r} = \frac{1}{1 + (\tau_r/\tau_{nr})} \quad . \quad (2.26)$$

Eqn. (2.26) implies that when the nonradiative recombination rate is higher, i.e. when  $\tau_r \gg \tau_{nr}$ , radiative recombination efficiency is relatively smaller. On the other hand, radiative recombination rate is higher, i.e. when  $\tau_{nr} \gg \tau_r$ , radiative recombination efficiency is relatively large [2].

## **CHAPTER III**

### **EXPERIMENTAL TECHNIQUES**

#### **3.1 Introduction**

In this chapter crystal growth procedure, starting from choosing the crucible to growth of single crystal ingots is presented. In addition, ion implantation and annealing processes will be mentioned. Finally, the details of photoluminescence measurements and used devices during the experiments are presented.

#### **3.2 Crystal Growth by Bridgman-Stockbarger Technique**

In order to grow a crystal using Bridgman technique a growth ampoule (crucible) is used. Determining a suitable crucible is an important factor for growing a crystal since it affects the physical properties of the grown material such as its purity, type and orientation. There are many criteria needed to be considered before choosing a convenient crucible for specific grown materials. Crucible material should have the following properties: [67, 69].

- The crucible should not react with the melt. Otherwise, this results in contamination of crystal which will be grown in the crucible and obtain a crystal which is different from the crystal which we desire.
- Coefficient of thermal expansion of the crucible should be smaller than that of grown crystal. Otherwise, the crystal expands much more than the crucible and this gives rise to cracks in the crucible.

- The crucible's melting point should be larger than the crystal's melting point.
- The crucible should have lower thermal conductivity than the growing crystal in order to obtain more appropriate shape of liquid-solid interface isotherm to get better quality crystals.

Other important factors affecting grown crystal type and quality are the crucible's shape and size. The Bridgman crucibles have usually circular cross section and pointed bottom shape. The crucibles with pointed tips lead to grow one nucleation at the pointed end and provide to obtain single crystals during the growth process [69]. It has been shown that by using large ampoules, it is possible to obtain polycrystalline ingots whose diameters are larger than 10 mm. On the other hand, for small ampoule diameters (diameter <10 mm) it was observed that monocrystalline ingots are grown [88]. Thus, the bottom shape and the diameter of the crucible determine whether the crystal growing in the ampoule is a single crystal or a polycrystalline. Fig.3.1 shows some pointed bottom crucibles with different diameters.



Fig.3.1. Some pointed bottom crucible with different diameters

Considering all these criteria, in our laboratory GaSe and InSe single crystals ingots have been grown in pointed bottom quartz crucibles whose dimensions have been 10-16 mm diameter, 100 mm length, and with 1.5 mm wall thickness [89, 90].

In order to grow high quality crystals, it is also important to clean crucible since it is possible for crucibles to be contaminated by surface dust, grease and inorganic chemicals. To remove these, a convenient cleaning process must be performed. For cleaning quartz crucibles used in growing GaSe and InSe ingots, a special procedure have been used [89, 90]. After the cleaning process, the stoichiometric quantity of 4N purity Ga and Se for GaSe and 4N-pure In and Se in the ratio of 52% In and 48% Se for InSe have been prepared [89, 90]. Then, the prepared stoichiometric Ga and Se and non stoichiometric In and Se have been loaded into the crucibles. Finally, in order to synthesize these compounds, the quartz ampoules have been put into a constant temperature furnace (Lindberg). Crucibles are heated gradually up to 1050 °C and kept for four days in order to complete the reaction [89] while for synthesis of InSe the furnace has been heated slowly up to 750 °C for 12 hours [90]. In order to satisfy the homogeneity during the heating process, the ampoules have been shaken [89, 90].

Before mentioning the crystal growth by Bridgman-Stockbarger method, it is necessary to know how Bridgman-Stockbarger system works. In order to grow GaSe and InSe ingots, Crystalox MSD-4000 model three-zone Vertical Bridgman–Stockbarger system shown in Fig.3.2 have been used in the Crystal Growth Laboratory of Physics Department at METU [89, 90].

Bridgman Stockbarger system mainly consists of four parts [91]. One of these units is furnace system whose schematic diagram is shown in Fig.3.3. This system has three independent heating zones each of which is 150 mm long. In order to provide temperature control inside the Bridgman furnace three thermocouples are placed at the center point of each zone. In addition, there are two more thermocouples. One of them indicates the temperature at the bottom of the crucible and the other is present to prevent overheating in which case the whole system shuts down automatically with an alarm light. Another part of the Bridgman-Stockbarger system is crucible translation unit (CTU). This unit is mounted under the worktop of the furnace. By the help of this unit, the loaded crucible is moved downward and upward with a desirable speed. Third part of the Bridgman apparatus is furnace temperature control



Fig.3.2. Bridgman Stockbarger System in the Crystal Growth Laboratory of Physics Department at METU

unit (TCU). In this unit, the temperatures of each three furnace zones are independently controlled by a programmable controller and they are kept at a constant value within an accuracy of about  $\pm 0.1$  °C. The last part of the system is chart recorder. With a 4-pen chart recorder in the control console, monitoring the temperature of three thermocouples is provided. Each of four channels displays temperature change ranging from 0-1200°C. Furthermore, data obtained from the channels can be stored [91].

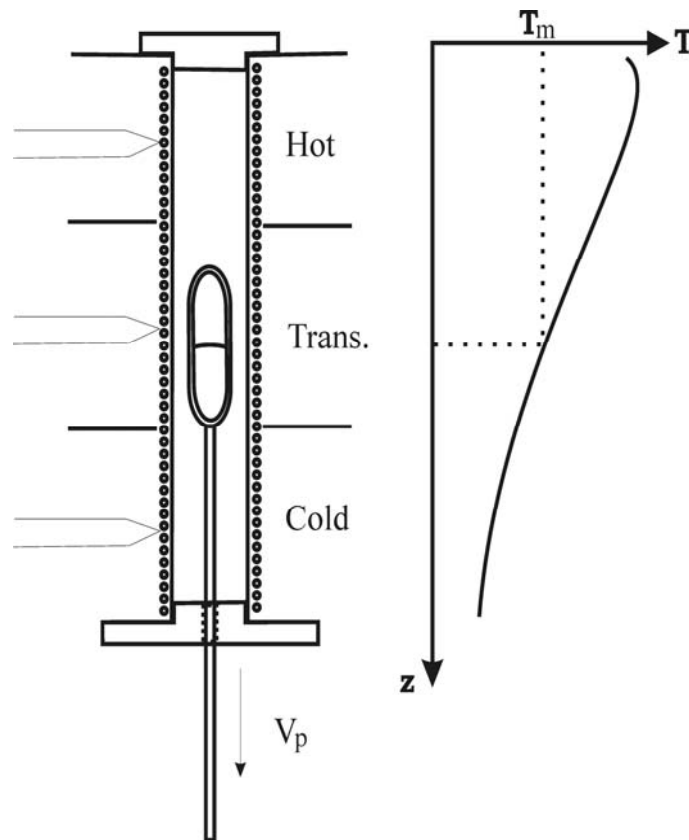


Fig.3.3. Schematic diagram of furnace system and the ideal temperature distribution along the axis of a cylindrical crucible

Now, our knowledge about the system is sufficient to start to mention the crystal growth process. Firstly, the crucible is placed into the upper part of the Bridgman furnace. Since each material is grown under temperature conditions specific to material, in order to grow crystals by using this technique, the temperature of each zone must be adjusted according to the growing material. For instance, GaSe ingots have been grown by setting the temperature of each zone to 1030, 920, and 750°C, while for InSe crystals the temperature settings of each zone have been 750, 450, and 250 °C for the top, middle and bottom zone, respectively [89, 90]. In addition to temperature profiles, lowering rate is an important parameter so as to grow crystals with high quality. Cardetta et al. in ref. [88] have studied the effect of the lowering speed on the grown crystals and they can be grow very good GaSe crystals with a lowering rate range of about 0.2 to 1.0 mm/h. GaSe and InSe crystals which we used in PL measurements have been grown with the transition speed 1.0 mm/h, too. The

growth time of GaSe ingot was 105 hours, while for InSe it took nearly 160 hours. Then, the translation of the crucible is stopped and temperatures are adjusted to reach the room temperature. Finally, in order to perform PL experiments and implantation process, we prepared four samples of each of GaSe and InSe by cleaved the crystals parallel to the layers, i.e., perpendicular to the c-axis with a razor blade.

### 3.3 Ion Implantation and Annealing Processes

As it was mentioned in previous chapter, ion implantation is a doping technique introducing high energetic ionized dopant atoms into a target material by bombardment with ions. A schematic representation of an ion implanter is given in Fig.3.4. In this process firstly, gas, liquid or solid source are ionized by tungsten filament. Secondly, the ions pass through the analyzing system which eliminates unwanted ions by the help of magnets. Thirdly, the selected ions are accelerated to high energies (from keV to MeV) by electric field in the acceleration tube and they enter the scanning system which distributes the ions uniformly over the target material. Finally, accelerated ions reach the target [70].

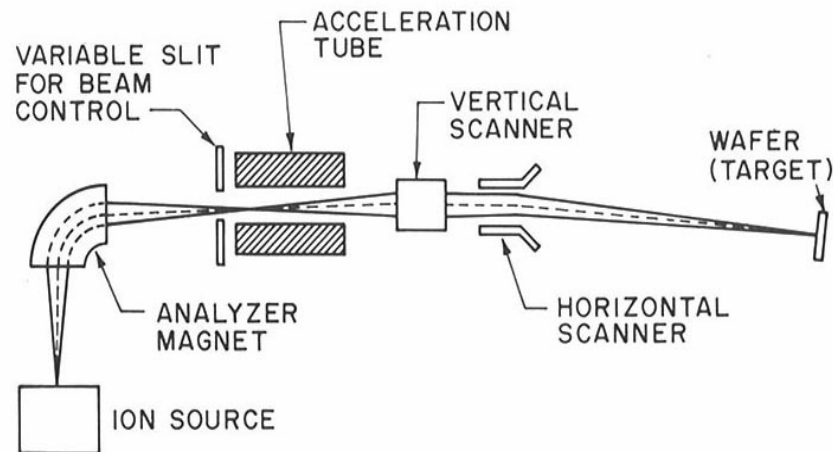


Fig.3.4. Schematic diagram of an implantation system [70]

In this study, a Varian Model 200-DF4 type implanter, which is founded in Physics department at METU, was used in order to implant our GaSe and InSe samples with Ge ions. Implantation system used is shown in Fig.3.5.



Fig.3.5. Ion implantation system in METU Physics department

For Ge implantations, one GaSe and one InSe sample was placed into the implanter such that the surface of each sample perpendicular to  $c$  axis will be bombarded by Germanium atoms. Then, the energy and dose of the ion beams were adjusted 100 keV and  $1 \times 10^{13}$  ions/cm<sup>2</sup>, respectively and Ge ions was implanted into the samples. This process was performed with doses  $1 \times 10^{14}$  and  $1 \times 10^{15}$  ions/cm<sup>2</sup> for other samples. As a result, one set of Ge implanted GaSe and one set of Ge implanted InSe samples with doses  $1 \times 10^{13}$ ,  $1 \times 10^{14}$ , and  $1 \times 10^{15}$  ions/cm<sup>2</sup> was obtained.

As it is stated before, during the implantation, the energetic ions damage the sample material due to the collisions of ions with nuclei and electrons of atoms in the sample. In order to reduce implantation induced damages, annealing process is carried out. Using this process, it is possible to recover damages partially in the structure. In this study, to investigate the effect of annealing on PL spectrum, firstly, PL signals of as grown and Ge implanted GaSe and InSe samples were measured. Then, annealing was performed in argon medium for  $1 \times 10^{15}$  ions/cm<sup>2</sup> Ge implanted

GaSe and InSe samples at 500 °C for 20 minutes. Samples were then cooled in argon medium with setting the furnace to room temperature. After that, for these samples photoluminescence measurements were repeated. In order to distinguish samples easily, some appellation related to the sample properties were chosen as listed in Table 3.1.

Table 3.1. Samples used in PL measurements and their donated names

	Implantation doses	Not annealed	Annealed
GaSe	-	GaSe-0	---
	$1 \times 10^{13}$ ions / cm <sup>2</sup>	GaSe-1	---
	$1 \times 10^{14}$ ions / cm <sup>2</sup>	GaSe-2	---
	$1 \times 10^{15}$ ions / cm <sup>2</sup>	GaSe-3	GaSe-3A
InSe	-	InSe-0	---
	$1 \times 10^{13}$ ions / cm <sup>2</sup>	InSe-1	---
	$1 \times 10^{14}$ ions / cm <sup>2</sup>	InSe-2	---
	$1 \times 10^{15}$ ions / cm <sup>2</sup>	InSe-3	InSe-3A

### 3.4 Photoluminescence Measurements

#### 3.4.1 Photoluminescence System

The basic experimental set-up consists of three main components: (1) an excitation light source whose photon energy exceeds the band gap of the material to be examined; (2) a cryostat system in order to maintain the samples at cryogenic temperatures while allowing the source light to reach the surface of the sample; and (3) a detection system to disperse and analyse the photons which are emitted from the sample. In addition to these three parts, so as to direct the laser onto the sample and focus the emitted signals onto detection system lenses and mirrors are used. These parts will be explained separately in this section. The photoluminescence system used during the measurements is indicated in Fig.3.6.

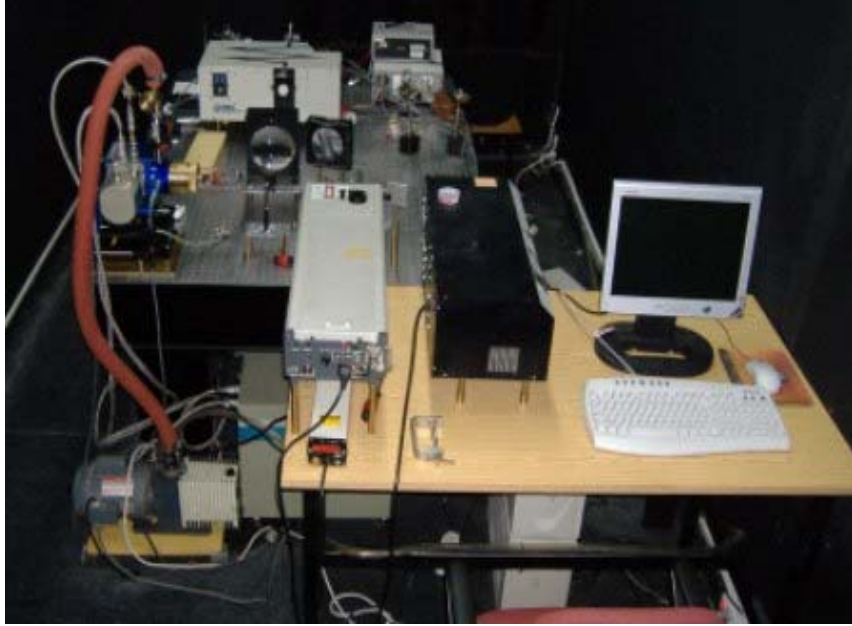


Fig.3.6. Photoluminescence set up in Department of Physics at METU

In photoluminescence experiments, light source, whose power is sufficient to obtain PL signals from the sample, can be any laser in order to provide a beam of photons with energy higher than the band gap of the studied material. In the experiments, a Nd:YAG, Neodymium doped yttrium aluminium garnet ( $\text{Nd:Y}_3\text{Al}_5\text{O}_{12}$ ), laser was used to excite the samples. It is operated with a radiation at 532 nm and producing photons with energies 2.33 eV.

It is known that for the samples held below room temperature better PL spectra (i.e. sharper and more identified peaks) are obtained because cooling prevents thermal ionization of the impurities and reduces lattice vibration which induces spectral broadening of luminescence bands. Therefore, most photoluminescence measurements are performed at low temperatures. In order to measure temperature dependent photoluminescence signals, cooling systems such as cryostats cooled to liquid nitrogen operated from 77 K to 300 K and liquid helium cooled cryostats which can be cooled down to 4K are used. In this study, for photoluminescence measurements, a “CTI-Cryogenics M-22” closed-cycle helium cryostat that cools the samples from 475 K down to 15 K was used. In general, the system reaches base temperature typically in 40-60 minutes depending on mounted mass on the cold

finger [92]. In order to obtain PL spectra at a desirable temperature the sample's temperature should be adjusted by a temperature controller. In order to manage this, a Lake Shore 330 temperature controller was used. It has typically  $\pm 0.5$  K control accuracy [93] and gives the temperature with a temperature sensor which is fitted backside of the holder.

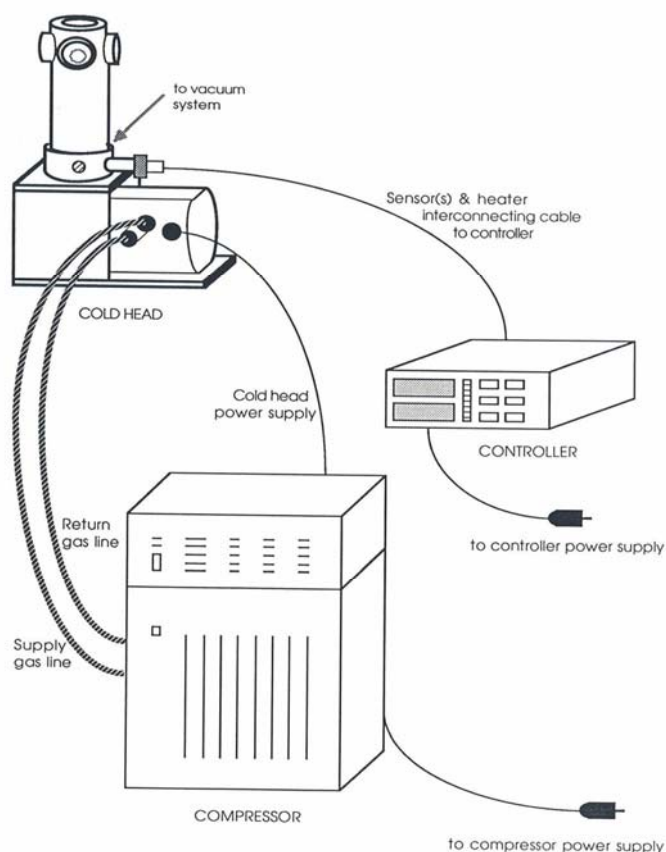


Fig.3.7. “CTI-Cryogenics M-22” closed-cycle helium cryostat system [92]

In order to direct the laser light on to the sample two Newport 10D10AL.2 mirrors and an Oriel 17960 mirror were used. The emitted photoluminescence signals were focused by two convex lenses onto the entrance slit of the monochromator. Moreover, in order to eliminate exciting light from the collected light a Notch filter was placed in front of the monochromator. In addition, Model 77721 fixed slit housing was used with mounting of Oriel 1.5 inch (47 mm) series to set a limit on the resolution of spectrum. The height of the slit is 15 mm and it has micrometer spindle

whose 10  $\mu\text{m}$  movement corresponds to 10  $\mu\text{m}$  change in slit width. In our measurements, it was 1 mm for all samples.

Monochromator spectrally resolves the signals, transmitting a selectable narrow band of wavelengths of light chosen from a wider range of wavelengths coming from the sample. The wavelength range which is transmitted from the monochromator varies with the choice of grating consisting of a substrate with a large number of parallel grooves in its surface and overcoated with a reflecting material such as aluminium. In this study, we used an Oriel model 77700a *MS257*<sup>TM</sup> monochromator and spectrograph (Fig.3.8). The device can be operated with four different gratings. Two parameters, space between two grooves and obtained peak efficiency, for each grating is given in Table 3.2 [94]. The monochromator was controlled through RS232 port of the computer by using programs written in LABVIEW.

Table 3.2. Groove spacing and peak efficiency for each grating [94]

	Grating 1	Grating 2	Grating 3	Grating 4
Groove spacing (Lines/mm)	1200	300	150	75
Peak % Efficiency	80	80	95	80

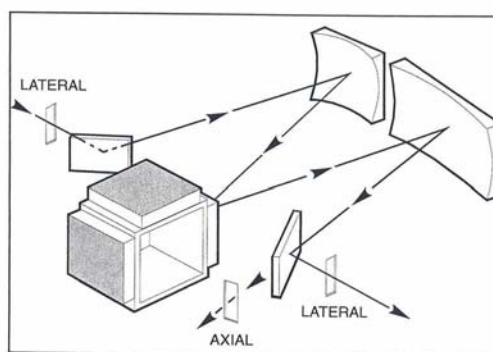


Fig.3.8. Diagram representation of *MS257*<sup>TM</sup> as a monochromator [94]

In order to detect photoluminescence signals, a Hamamatsu C7041 multichannel detector with S7031-1008 serial CCD (Charge Coupling Device) image sensor with

1044 x 256 number of pixels was used. It incorporates a low-noise driver/amplifier circuit which reliably operates by input of simple external signals [95].

### **3.4.2 Measurements by the PL System**

The analysis of semiconductor materials with photoluminescence systems includes various measurement configurations. In one of them, the wavelength of the incident light is fixed and the intensity of the emitted PL signals over a specific range is monitored. On the other hand, in another analysis method with photoluminescence system, the wavelength of the incident radiation is changed and the wavelength of the analyzing system is fixed. In addition to these analysis methods, there are also time-resolved photoluminescence measurements in which the photoluminescence intensity resulting from the recombination of electron and holes in the semiconductor is measured as a function of time delay following the excitation pulse [2]. In our measurements, we fixed the wavelength of the incident laser radiation and monitored and recorded the luminescence coming from the sample which was held at different temperatures.

In order to take measurements, firstly, the sample was mounted to a holder provided by Cryophysics and placed into the cryostat. Then, the temperature sensor is fitted at the holder's backside and the quartz head was closed. A vacuum pump was operated in order to create a vacuum atmosphere inside the head. After the vacuum meter indicated  $3 \times 10^{-2}$  torr, cooling process was started by adjusting the temperature controller in order to cool the system at the lowest temperature as possible. Then, we waited for the system to reach this temperature. After that, laser radiation was directed onto the sample at an angle of  $45^\circ$  with through the mirrors and the system was adjusted in order to focus luminescence emitted from the sample onto the entrance slit of the monochromator. The spectra were recorded on a computer equipped with a SCSI card for the CCD. Also, data acquisition was done by using a special computer program. The observed Gaussian like peak center energies and intensities were determined by using Peak Fit (Version 4) program while excitonic peak center energies and intensities were determined by using Origin Pro 7.0 program.

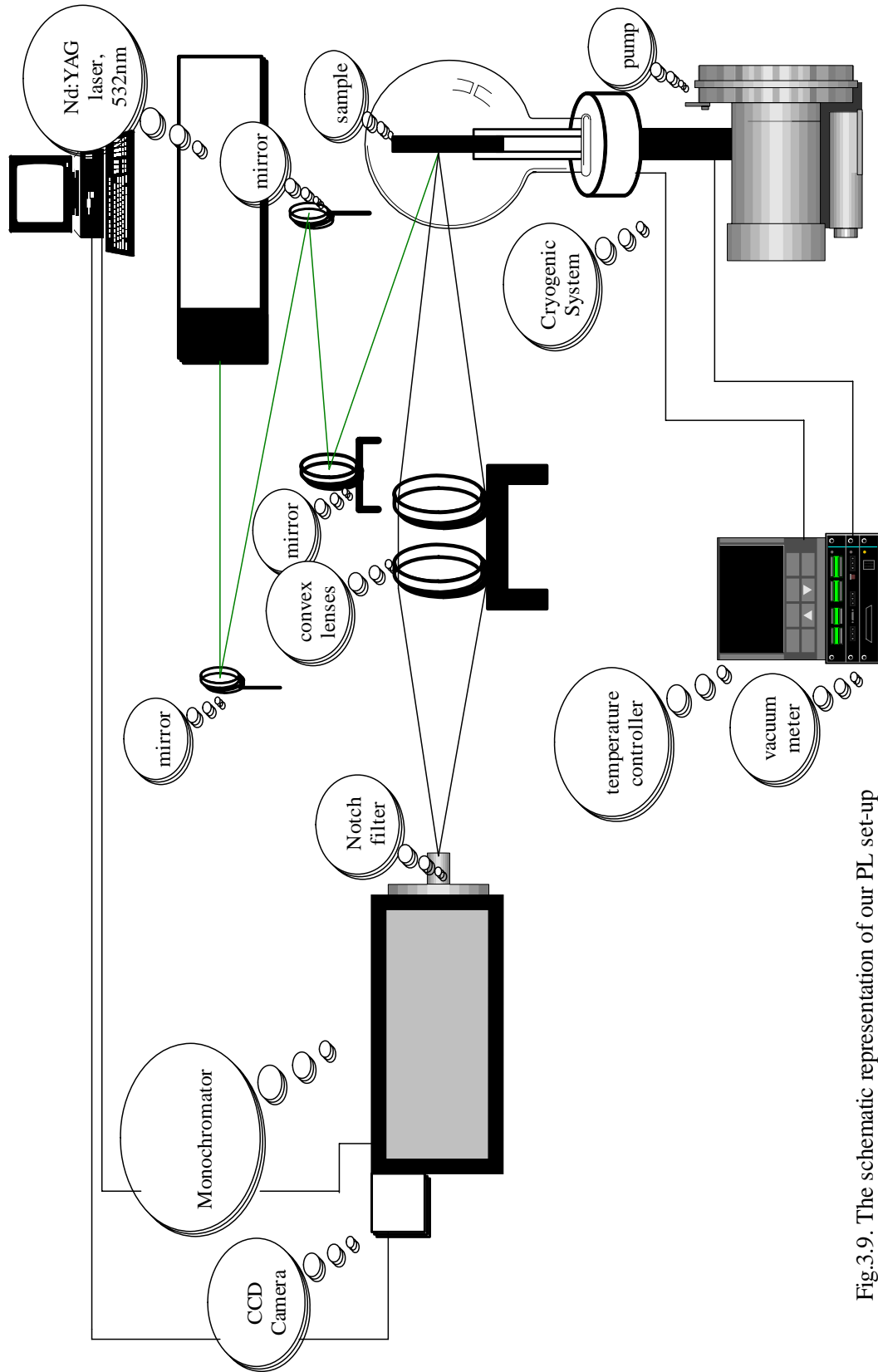


Fig.3.9. The schematic representation of our PL set-up

## CHAPTER IV

### RESULTS AND DISCUSSIONS

#### 4.1 Introduction

In this chapter, the results on temperature dependent photoluminescence measurements for as grown and Ge implanted GaSe and InSe crystals with doses  $10^{13}$ ,  $10^{14}$  and  $10^{15}$  ions/cm<sup>2</sup> and also  $10^{15}$  ions/cm<sup>2</sup> Ge implanted and annealed GaSe and InSe crystals are given in details.

For this study, four different GaSe and InSe samples were used. Samples were obtained by cleaving the grown ingot parallel to the plane which is perpendicular to c-axis. Then, Ge ions were implanted to the three samples with doses  $10^{13}$  ions/cm<sup>2</sup> (GaSe-1 and InSe-1),  $10^{14}$  ions/cm<sup>2</sup> (GaSe-2 and InSe-2), and  $10^{15}$  ions/cm<sup>2</sup> (GaSe-3 and InSe-3). After that, PL spectra of as-grown (GaSe-0 and InSe-0) and Ge implanted samples were measured from the temperature to which cryostat can cool down up to the temperature no PL signals can be obtained.

#### 4.2 PL Analysis of As-grown GaSe

Fig.4.1 shows excitonic and non-excitonic PL spectra obtained from the GaSe-0 sample in between 575-850 nm and 32-85 K at constant excitation intensity of 429.9 mW/cm<sup>2</sup>. In the spectrum obtained at 32 K, three emission bands centered at 590.2 nm (2.101 eV, A-band), 674.9 nm (1.837 eV, B-band), and 759.6 nm (1.632 eV, C-

band) were observed. A-band is relatively narrow while the remaining two lines are broader and extends toward lower energies.

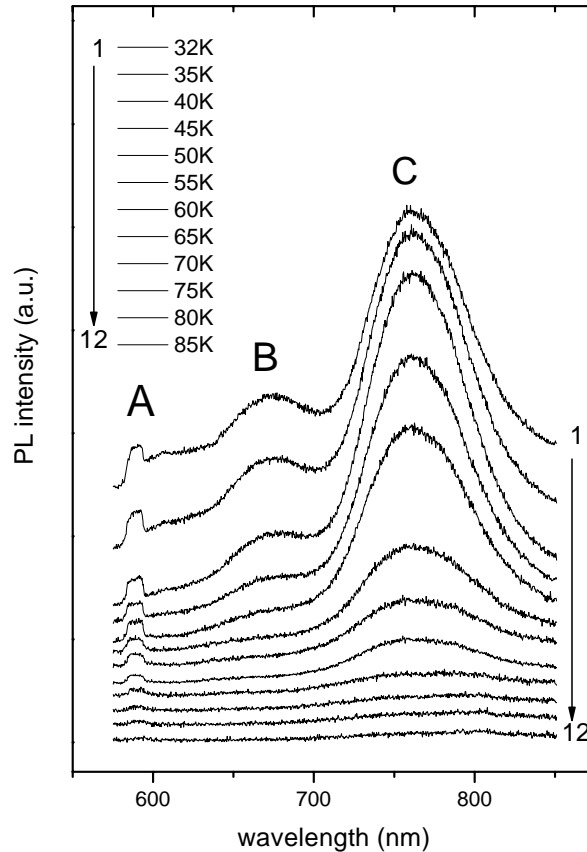


Fig.4.1. Temperature dependence of emission spectrum obtained from GaSe-0 single crystal in the temperature range of 32-85 K

As it can be seen, both PL peak intensities and positions changed as a function of increasing sample temperature. The variations of the peak intensity of all three bands with respect to temperature were plotted in Fig.4.2. As the temperature was increased, a decrease in the PL emission intensity of the two high energy (short wavelength) peaks was observed, whereas the intensity of the third band increased in the narrow temperature range 32-40 K, followed by a decrease of the emission intensity. In the low temperature region, PL intensities of the A- and B-bands decreased slowly. Above 50 K for A-band and 40 K for B band, an increase in the rates of the intensity was observed probably due to the intensive thermal quenching

process. The activation energies,  $E_a$ , for all three bands have been obtained by using the equation:

$$I \propto \exp(E_a / k_B T) \quad (4.1)$$

where  $I$  is the emission intensity,  $E_a$  is activation energy and  $k_B$  is the Boltzmann's constant. The semi logarithmic plots of the emission band intensities as a function of reciprocal temperature gave straight lines for all three bands in the 50-75 K, 40-70 K, and 50-85 K regions for A-, B-, and C- bands, respectively. From the slopes of the lines, activation energies of the three peaks were found to be 0.019, 0.017 and 0.031 eV for A-, B-, and C-bands, respectively.

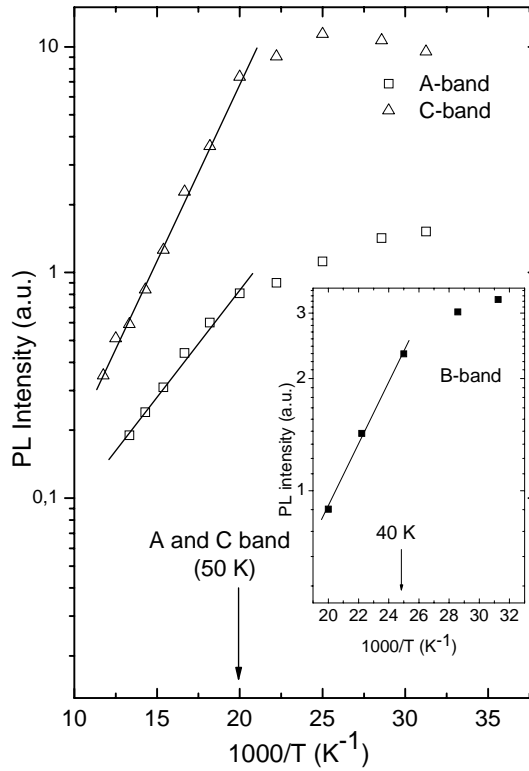


Fig.4.2. Temperature dependence of the A, B, and C bands (The arrows shows the starting points of intensive thermal quenching.)

Relatively narrow lines located at the high energy part of the spectrum have been observed by many groups and considered to be excitonic origin [24, 25, 27, 31, 32]. Center and activation energy of A-band agree with values given in the literature. This

band have been observed at 591.039 nm by Dobynde et al. [27], at 591 nm by Capozzi [24, 32], at 590.476 nm by Shigetomi et al. [31]. Moreover, J. P. Voitchovsky et al. [25] found 20 meV for the activation energy of their observed peak centered at about 590 nm. All these bands have been attributed to direct free exciton. Since our values are in very good agreement with previously obtained ones, we considered that A emission band at 590.2 nm to be due to the recombination of direct free exciton. The fine structure around 590.2 nm may be due to various possibilities of stacking layers of GaSe crystals grown by Bridgman method [96]. Because of low resolution (about 0.29 nm for grating 2) of CCD detector used in this study, direct free excitons from excited states  $n=2$  and  $n=3$ , which have been observed in the higher energy part of the ground state direct free excitonic band [25, 28], may not be detected clearly. Direct energy band gap of GaSe-0 sample was evaluated by adding the free excitonic band energy to their activation energy. It was found to be 2.12 eV at 32 K. This value also agrees with the previously obtained values [21].

Because B and C-band were located on the lower energy side of the excitonic emission, these PL peaks may be related to impurity levels localized in the forbidden energy gap [33]. In order to understand radiative recombination mechanisms, resulting in B and C band emissions, temperature dependence of the band energies is plotted (Fig.4.3). It was observed that the peak energies decrease with increasing temperature. Also, the variation of the band gap energy of GaSe as a function of temperature was plotted by linear extrapolation using the band gap values given in ref. [21] with the assumption that the variation is linear. The negative shift of the bands may result from band to impurity or donor acceptor transitions [60]. However, because the energy variation rates of both bands are different from that of the band gap, we considered that B and C band are not due to the band- impurity recombination [33]. Since GaSe-0 sample is p-type, which has been found from Hall measurements [89], we assumed that the activation energies of the two lower energy bands are associated with acceptor levels. In other words, we consider that B and C band peak emissions were related to the acceptor levels located at 0.017 and 0.031 eV, respectively. Similar assumptions have been made for p-type as grown and Cu and Ag doped p-type GaSe crystals [30, 32, 39]. To our knowledge, the activation

energy of 0.017 eV that we obtained from the B band was not observed before. From the temperature dependent PL intensity of undoped p-type GaSe crystal, acceptor level of 0.014 eV has been found by ref. [30]. Moreover, an acceptor level located at 0.030 eV above the valence band has been obtained from as-grown GaSe crystals [29]. The activation energy of C-band that we observed is in fair agreement with this result.

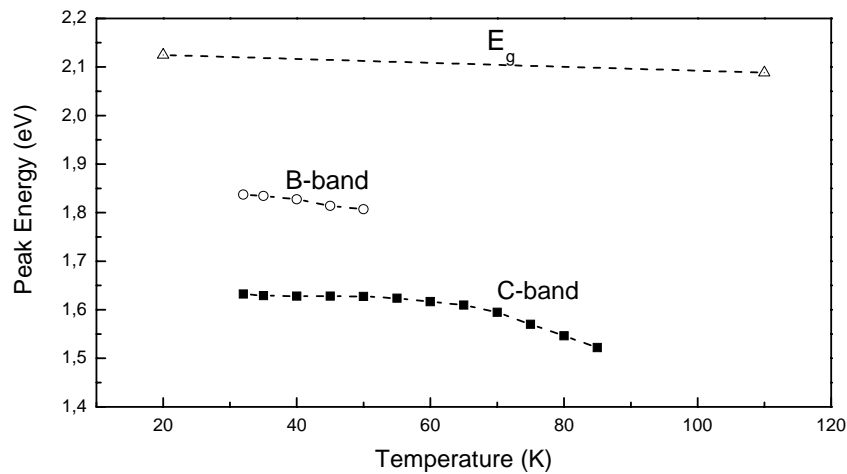


Fig.4.3. Temperature dependence of the peak energies of B and C bands (The dashed line shows the variation of direct band gap of GaSe [21].)

The sum of the B band energy of 1.837 eV and thermal quenching activation energy of 0.017 eV was smaller than the value of the band gap energy. Since donor levels in p-type GaSe associated with the defects in dislocations or stacking faults may form [31], the B emission band may be considered to arise from the transitions from a donor level at 0.266 eV below the conduction band to the acceptor level, located 0.017 eV above the valence band (Fig.4.4.). The value of donor level of 0.266 eV agrees with the previously found one (0.264 eV) in as grown GaSe obtained from temperature dependence of the PL intensity [30]. Similarly, the sum of emission energy of 1.632 eV and 0.031 eV activation energy of the C band again does not agree with the band gap of the sample. C. Manfredotti et al. and V. Capozzi have found deep donor levels at 0.421 and 0.416 eV [24, 97]. If GaSe-0 sample has impurity donor level at 0.457 eV below the conduction band, the radiative process resulting in C band emission may be considered to the transition from the donor level

at 0.457 eV to the acceptor level at 0.031 eV (Fig.4.4.). This donor level has not been reported so far, according to our literature survey. These moderately deep donor and shallow acceptor levels obtained by us may be associated with the stacking faults or dislocations, which are easily produced in the material due to nature of weak van der Waals forces between the layers [98, 45]. In addition, Micocci et al. have reported that Se vacancies behave as donor in GaSe [99]. Moreover, it is possible that some impurities might be present between the layers [45]. In the proposed scheme (Fig.4.4), two shallow acceptor levels  $a_1$  and  $a_2$  located at 0.017 and 0.031 eV above the top of the valence band are presented. From the observation of two PL bands, two deep donor levels  $d_1$  and  $d_2$  located at 0.266 and 0.457 eV below the bottom of the conduction band are introduced into direct forbidden energy gap of GaSe-0 sample. This diagram may permit to explain the thermal quenching behavior of non-excitonic bands in GaSe-0 sample, where the intensity of C-band increases in the temperature range between 32 and 40 K. To our knowledge, such an increase in the intensity of the emission bands in GaSe has not been reported before this study. However, increase in the intensity of a band with increasing temperature has been observed in Mg-doped GaN epilayers grown on sapphire substrates [100], TlGaS<sub>2</sub> layered crystal [101] and Ga<sub>4</sub>Se<sub>3</sub>S [102]. We consider during the quenching of B band, holes might be thermally released from the acceptor level  $a_1$  to the valence band. Then, the thermally released holes may be captured by the acceptor level  $a_2$ . As a result of this, increase in the intensity of C-band was observed in a small temperature range.

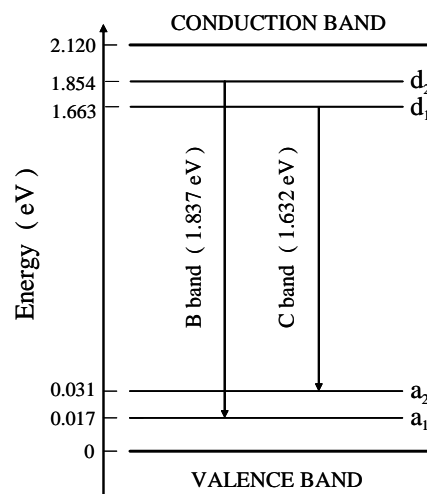


Fig.4.4. Proposed energy diagram of the impurity levels in GaSe-0 sample at 32 K

### 4.3 PL Analysis of $10^{13}$ ions/cm<sup>2</sup> Ge Implanted GaSe

PL spectra of GaSe-1 in the 570-850 nm wavelengths and 25-110 K temperature range at the same excitation intensity are indicated in Fig.4.5. Four PL peaks centered at 590.2 nm (2.101 eV, A-band), 598.8 nm (2.071 eV, B-band), 668.4 nm (1.855 eV, C-band), and 762.5 nm (1.626 eV, D-band) were observed at 25 K. It is seen from the spectra that the observed band intensities and the positions changed as the sample temperature increased. While intensities of A, B, and C bands decreased with increasing temperature, D band showed an intensity behavior a little different than the other peaks. All bands showed varying degrees of red shift with temperature.

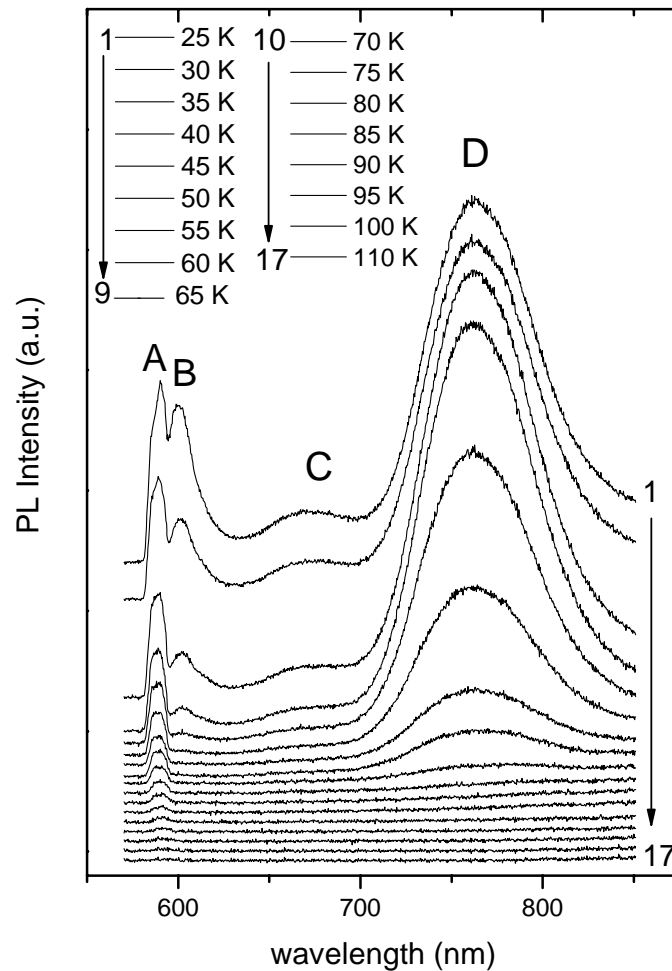


Fig.4.5. PL spectra of GaSe-1 sample a function of temperature

The semi logarithmic plot of the emission intensity of the all bands with respect to temperature was given in Fig.4.6 so as to clearly show the variation of the band intensities. All band intensities decrease with temperature (except for D). Above 45 K for A-band and 40 K for C-band, however, the peak intensities decreased at a much larger rate while D band intensity decreased from 25 to 30 K, an increase was observed between 30 and 35 K and this was followed by a decrease until it totally quenched. The experimental data for the temperature dependence of the emission intensities can be fitted by eqn. (4.1). The slopes of the lines indicated in the figure give the activation energies of emission bands. They were found to be 0.020, 0.049, 0.022, 0.028 eV for A, B, C, and D bands, respectively.

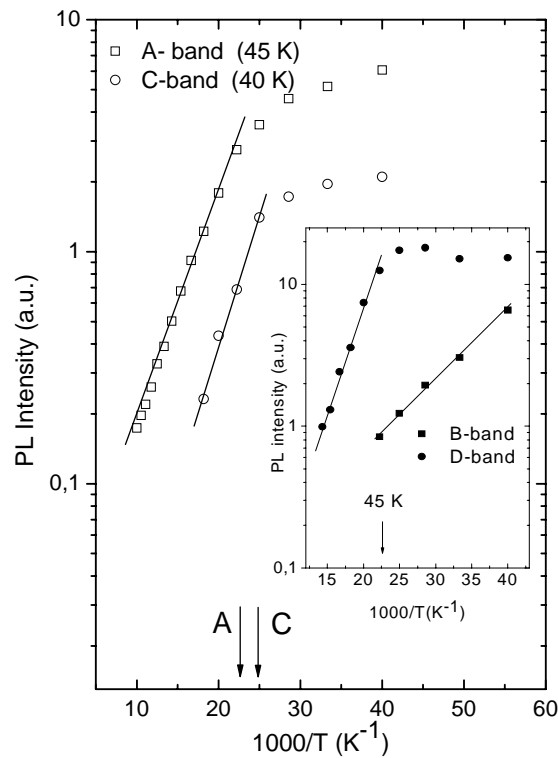


Fig.4.6. PL intensities of observed bands as a function of reciprocal temperature, the arrows show the starting temperatures of rapid thermal quenching.

Emissions related to excitons existed in the region from about 580 to 620 nm [29] and their peaks were narrow comparing with the other observed bands. Therefore, the origin of the A and B bands can be excitonic. According to our literature survey,

A band's activation energy of 0.020 eV was in exact agreement with the value of the activation energy of the direct free exciton and also there was a very good agreement between its center (2.101 eV) and that of the direct free exciton given in the literature [24, 25, 27, 31, 32]. Moreover, it was also observed in the PL spectrum of our GaSe-0 sample. Thus, A-band was attributed to the recombination of direct free exciton. Then, direct forbidden energy of the GaSe-1 sample was found to be 2.121 eV at 25 K. The results of Hall measurements showed that  $10^{15}$  ions/cm<sup>2</sup> Ge implanted GaSe sample is p-type [89]. Therefore, GaSe-1 sample, implanted with  $10^{13}$  Ge ions/cm<sup>2</sup>, assumed to be p-type. Therefore, obtained activation energies might be considered to be the acceptor levels located at 0.049, 0.022, 0.028 eV above the top of the valence band.

The energy position of the B-band centered at 2.071 eV was in very good agreement with direct bound exciton reported in ref. [29] in which a band at 2.078 eV has been observed. Moreover, S. Shigetomi et al. [31] and V. Capozzi [32] have reported an acceptor level located at 0.050 eV for Zn- and Cu-doped GaSe crystals, respectively. The activation energy of B-Band (0.049 eV) also agreed fairly with these data. Therefore, the origin of the B-band might be a direct exciton bound to acceptor level 0.049 eV above the valence band. The quenching of this peak as temperature increased might be attributed to the thermal freeing of the excitons from their acceptor level.

C and D bands were centered non-excitonic region of GaSe. Therefore, their emissions might be associated with impurity levels. Transitions resulting in these PL bands might be from the conduction band to acceptor level or from donor level to acceptor level. An acceptor level located at 0.031 eV above the valence band has been reported for Cu-doped GaSe crystals by ref. [32]. Moreover, V. Capozzi has been observed an acceptor level centered at 0.023 eV [24]. It is seen that there is a good agreement between acceptor levels obtained from our analysis and previously found results.

The variations of peak energy for C and D emission bands are shown in Fig.4.7. Both PL peak energies shifted towards red continuously. The magnitude of shift of C and

D-band energies were 0.025 and 0.022 eV. Since the decrease in the energies of the both bands was different, it was possible to say that the centers responsible for the observed recombinations were not the same, but similar.

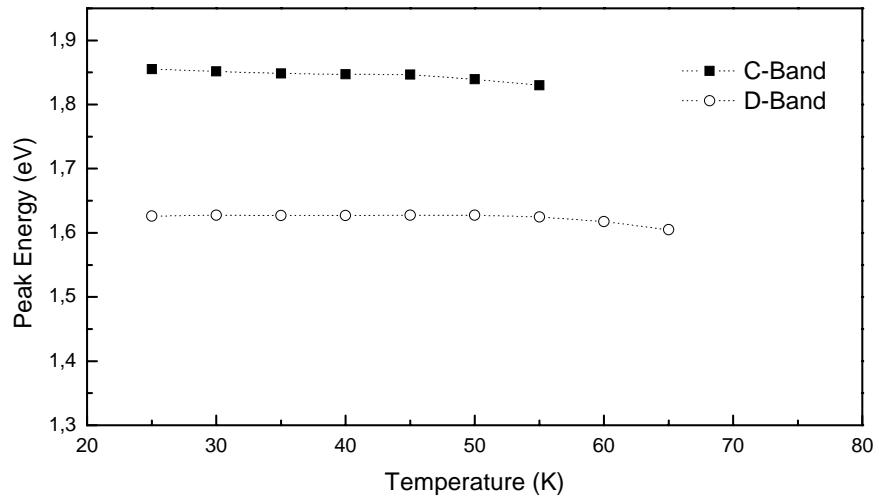


Fig.4.7. Temperature dependencies of C and D-bands peak energies for GaSe-1 sample

The sum of the C-band energy of 1.855 eV and the activation energy of 0.022 eV was smaller than the value of the band gap energy. Therefore, if GaSe-1 sample had a donor state located 0.243 eV below the bottom of the conduction band, the recombination mechanism resulting in C-band might be considered as transitions from the donor level at 0.243 eV to the acceptor level located 0.022 eV above the top of the valence band.

The donor level located at 0.467 eV was calculated for D-emission peak by adding the band energy of 1.626 eV to the thermal activation energy of 0.028 eV and subtracting the obtained value from the energy band gap of GaSe-1 sample at 25 K. As a result of this, D-band emission may be attributed to the recombination of the electrons located at 0.467 eV donor level and holes at the 0.028 eV acceptor level. It should be noted that acceptor and donor levels obtained from GaSe-1 sample was in agreement with the impurity centers found for GaSe-0 sample.

Recombination mechanisms for GaSe-1 sample which were found as a result of this analysis are presented in Fig.4.8. Two shallow acceptor levels  $a_1$  and  $a_2$  located at 0.022 and 0.028 eV above the top of the valence band are given in the figure. From the analysis of C and D-PL emission bands, two deep donor levels  $d_1$  and  $d_2$  located at 0.243 and 0.467 eV below the bottom of the conduction band were introduced in to the direct energy gap of GaSe-1 sample.

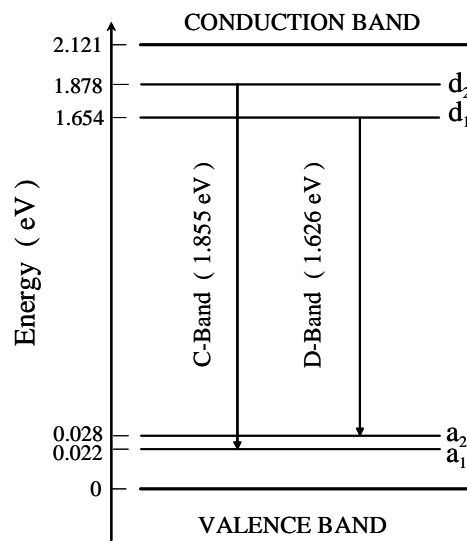


Fig.4.8. Proposed energy band diagram of luminescence related with impurity levels in GaSe-1 sample at 25 K

According to this diagram, it became possible to make some explanations about the increase in intensity of D-band with temperature in a small range, in which quenching of the C-band was observed. Similar to the case in GaSe-0, this might be due to redistribution of carriers as C- band was quenching rapidly.

#### 4.4 PL Analysis of $10^{14}$ ions/cm<sup>2</sup> Ge Implanted GaSe

Excitonic and non-excitonic luminescence spectra of GaSe-2 single crystal are shown in Fig.4.9 as function of temperature from 21 up to 80 K in the wavelength region 560-850 nm. We observed three emission bands with centers 589.6 nm (2.103

eV, A-band), 673.3 nm (1.842 eV, B-band), and 764.6 nm (1.622 eV, C-band) at 21 K. Since A-band is relatively narrow and located in the excitonic region of GaSe, A-band might be due to exciton related luminescence. Moreover, lower energy bands were broader and might be related to the impurity levels.

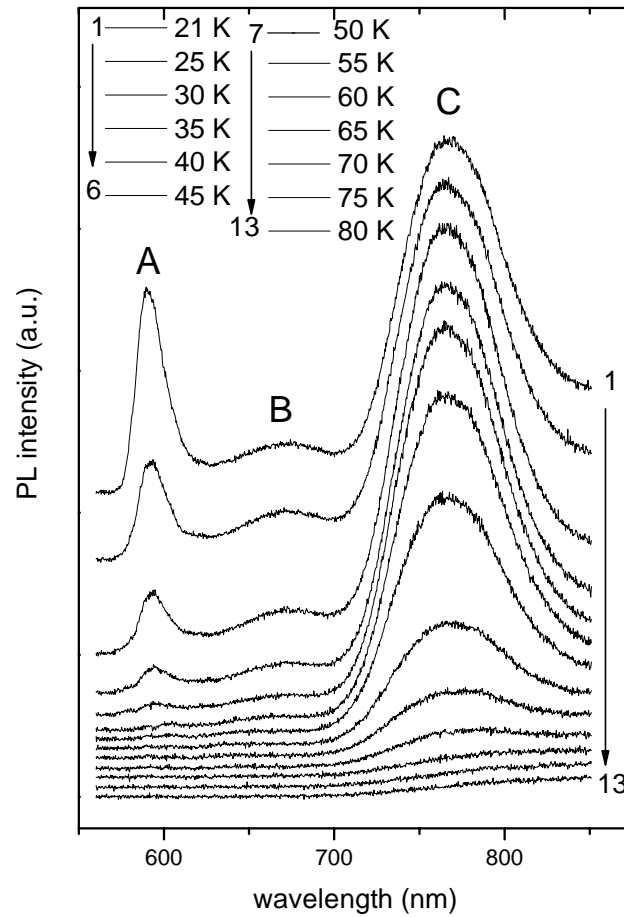


Fig.4.9. Temperature dependence of PL spectrum from GaSe-2 crystal

In order to show the variation of the PL intensity with temperature and to calculate activation energies of the peaks from the slope of the straight part of the data, semi logarithmic plot of the emission intensities as a function of the reciprocal temperature was plotted in Fig.4.10. As it can be clearly seen, the emission intensities of A and B bands decreased with increasing sample temperature. Rapid thermal quenching was observed at temperatures as low as 30 K for A-band and 35 K

for B-band. However, intensity behavior of C-band was different from the other bands. It increased between a small temperature range 21-30 K. A decrease was observed above 30 K but after 50 K this decrease was much sharper. The reason of the small increase in the PL intensity between 21 and 30 K could be the change of the distribution of carriers as B-band was quenching. Using the straight lines in the 30-40 K, 35-45 K, and 50-70 K regions, the activation energies of the bands were found as 0.018, 0.014, and 0.034 eV for A-, B- and C-band, respectively.

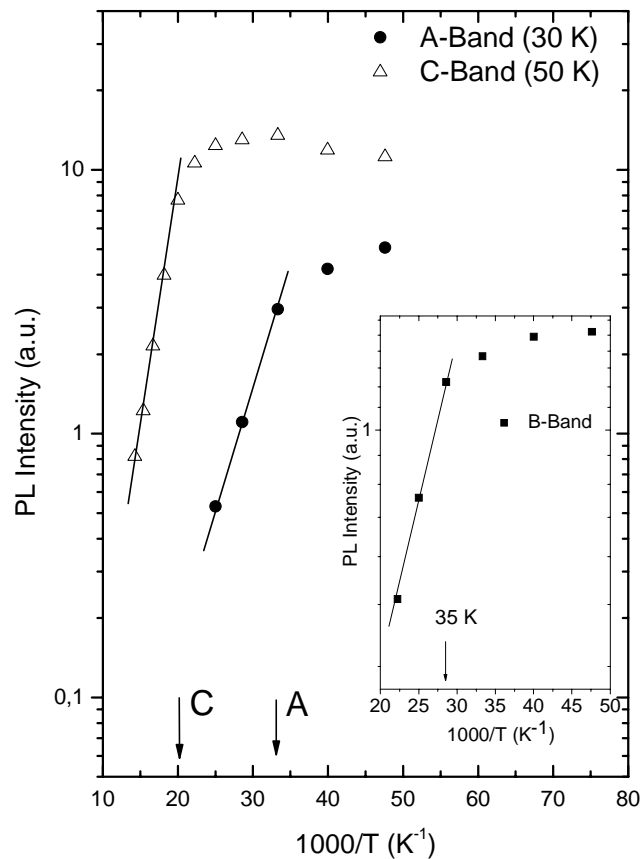


Fig.4.10. Temperature dependence of the peak intensity of A, B and C bands (The starting temperatures of rapid thermal quenching of the bands has been shown with arrows.)

The thermal activation energy and the location of the A-band were in good agreement with the results of the direct free exciton given in the literature [24, 25, 27, 31, 32]. Therefore, it was considered that A-band is due to the recombination of direct free exciton as in all our samples. Using the center and activation energy of the

direct free exciton, it was possible to calculate direct band gap energy of the GaSe-2 crystal. It was found as 2.121 eV at 21 K. Since GaSe-2 sample was assumed to be p-type, the activation energy of lower energy bands were donated to the acceptor levels at 0.014 and at 0.034 eV above the top of the conduction band. As it was stated, acceptor level of 0.014 eV has been obtained from undoped p-type GaSe crystal with the temperature dependent PL measurements reported in ref. [30]. In addition, acceptor levels centered 0.030 and 0.031 eV above the top of valence band have been found from as-grown and Cu doped GaSe crystals, respectively [29, 32].

It was found that recombination resulting in B and C bands might be related to acceptor levels centered at 0.014 and 0.034 eV, respectively. Emissions might be due to the transitions from conduction band to acceptor level or donor level to acceptor level. In order to find which the recombination mechanisms take place during the emissions, the temperature dependence of peak energies for B and C bands are plotted and indicated in Fig.4.11. Both band energies decreased with increasing temperature at different rates. The total red shifts were 0.03 and 0.087 eV for B and C band, respectively. The observed red shift for both bands is indicative of the donor acceptor pair recombination. Similar behaviour has been observed in many binary and ternary semiconductors [39, 103].

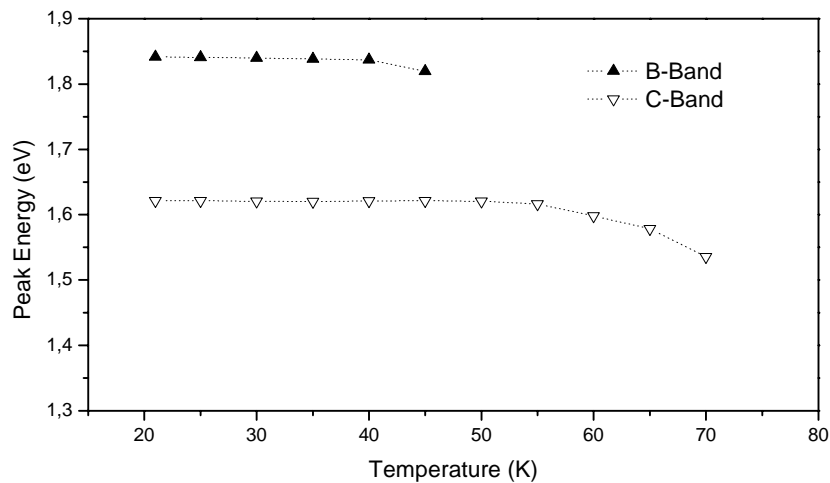


Fig.4.11. The variation of the peak center energies with temperature

Donor levels located 0.265 and 0.465 eV were calculated for B and C bands, respectively. Therefore, B band might be considered due to the transitions from the donor level centered 0.265 eV below the conduction band to the acceptor level, 0.014 eV above the valence band. Similarly, transitions between the donor level located at 0.465 eV and the acceptor level at 0.034 eV might be responsible for the C emission band. It was possible to show the results of transitions associated with impurity levels for GaSe-2 crystal with an energy band diagram (Fig.4.12). Two shallow acceptor levels  $a_1$  and  $a_2$  centered at 0.014 and 0.034 eV above the valence band were indicated. Using the results of two emission peaks, two deep donor levels  $d_1$  and  $d_2$  located at 0.265 and 0.465 eV below the conduction band were introduced in to the direct energy gap of GaSe-2 sample.

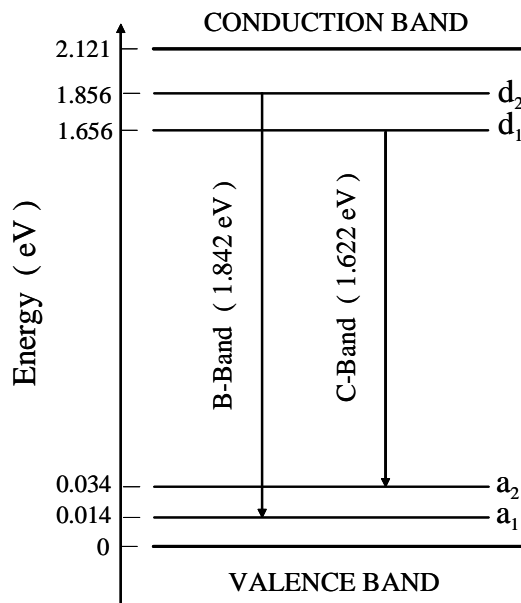


Fig.4.12. The energy band diagram indicating B and C transitions for GaSe-2 at 21 K

#### 4.5 PL Analysis of $10^{15}$ ions/cm<sup>2</sup> Ge Implanted GaSe

PL spectra obtained from GaSe-3 sample in the temperature range between 33 and 90 K and wavelength region 575-850 nm at constant excitation intensity, used in the

other measurements, is indicated in Fig.4.13. Four peaks located at 588.9 nm (2.105 eV, A-band), 610.1 nm (2.032 eV, B-band), 672.8 nm (1.843 eV, C-band), and 763.9 nm (1.623 eV, D-band) were observed at 33 K. It can be understood from the figure that the PL intensity and energy positions of the peaks changed with the sample temperature. As the temperature was increased, decrease in the observed peak intensities and the red shifts of the peak energies were observed.

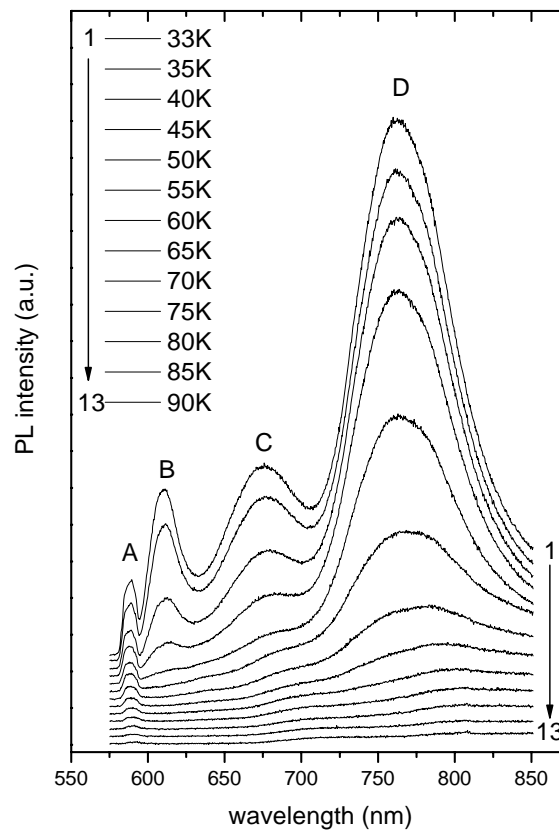


Fig.4.13. PL spectra of GaSe-3 as a function of temperature

In order to see the peak intensity variation with sample temperature semi logarithmic plot of the intensities of the bands with respect to temperature was shown in Fig.4.14. From the temperature range 33 to 45 K, intensity of A, C and D emission bands decreased slowly. Above 45 K, the peak intensities decreased at a larger rate due to the rapid thermal quenching. Using the straight lines in the 45- 85 K, 33-50 K, 40-50 K and 45- 85 K regions, the thermal activation energies of the peaks calculated as 0.019, 0.017, 0.025, and 0.025 eV for A, B, C, and D bands, respectively. Because

the activation energy and center of A-band was in very good agreement with the results given for the direct free exciton [24, 25, 27, 31, 32], it might be attributed to the recombination of the direct free excitons as the other samples. By adding the activation energy of the direct free exciton to the peak energy, direct band gap of the sample was found to be 2.124 eV at 33 K.

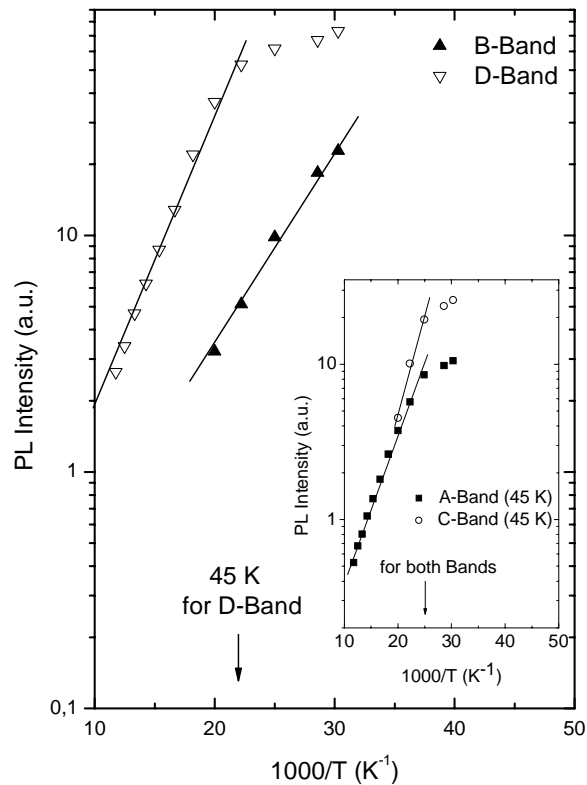


Fig.4.14. Temperature dependence of the observed peaks in GaSe-3 sample

B-band, located in excitonic region, was centered at 610.1 nm and has been previously observed at 609.2 nm by [24], 609.3 nm by [28], 609.2 nm by [32], and 609.3 nm [29]. The observed peak has been attributed to the radiative decay of indirect free exciton with emission of an  $A_1'$  phonon having energy of 15 meV. According to data obtained in this study, from the energy position of the B-Band and the phonon energy given above, the value of about 2.047eV for energy of indirect free exciton may be estimated [24]. Since the sum of the thermal activation energy of the B-band and indirect free exciton energy given above did not agree with the indirect energy gap, lying 25 meV below the direct one, B-band observed in this

sample might not be the previously observed peaks at about this location. However, because during the recombination process, the release of more than one phonon is possible [26], using the results of evaluations given above, B-band might be attributed to the indirect free exciton associated with three  $A_1'$  phonons.

The temperature dependence of peak energies for C and D emission bands was plotted in Fig.4.15. As temperature was increased, red shifts of the positions of both bands were observed. However, the magnitude of this shift was different for these two bands. The maximum of C-band lowered from 1.845 to 1.817 eV, while this shift is from 1.623 to 1.539 eV for D-band.

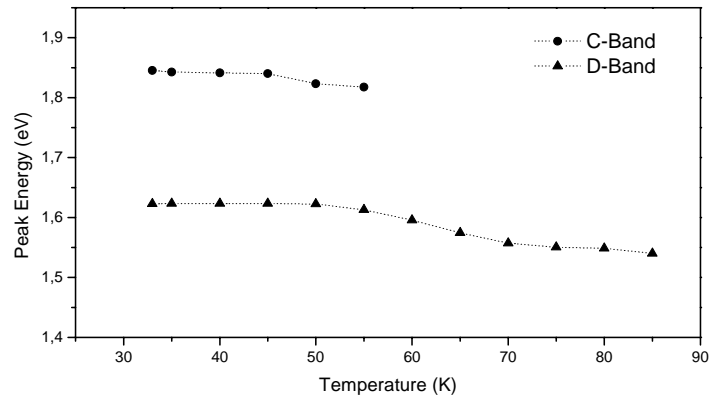


Fig.4.15. The variation of the observed impurity related peak energies with temperature in GaSe-3 sample

Because GaSe-3 is p-type [89], it might be considered that the activation energy of 0.025 was associated with an acceptor level. Therefore, it is possible to say C and D emissions might be related to the same acceptor level (0.025 eV). The acceptor level centered at 0.023 eV above the valence band has reported previously by Capozzi [24]. There is a very good arrangement between the activation energy estimated from GaSe-3 sample and the result obtained in ref. [24]. The sum of the C-band energy of 1.843 eV and the thermal activation energy of 0.025 eV is smaller than the value of the band gap energy. Thus, if GaSe-3 sample had a donor state located at 0.256 eV below the bottom of the conduction band, the recombination mechanism giving rise to C-band might be considered to be due to transitions from the donor level at 0.256

eV to the acceptor level located 0.025 eV above the valence band. Similarly, the donor states at 0.475 eV was found for D band. As a result, D emission peak might be due to the transition from the donor level at located 0.476 eV to the acceptor level at 0.025 eV.

The analysis of the observed peaks as a function of the temperature permitted to propose a possible scheme for the donor-acceptor levels located in the forbidden gap of the GaSe-3 crystal. These levels are involved the radiative recombination of the photoexcited carriers observed in the sample. A shallow acceptor level  $a_1$  located at 0.025 eV is shown in Fig.4.16. Moreover, from the analysis of impurity related emission bands, three deep donor levels  $d_1$  and  $d_2$  located at 0.475 and 0.256 eV below the conduction band are introduced into the direct forbidden energy gap of GaSe-3 sample.

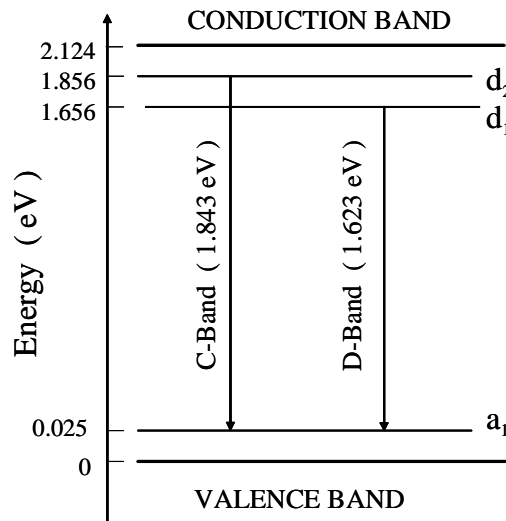


Fig.4.16. The proposed energy band diagram for the observed impurity related luminescence in GaSe-3 at 33 K

#### 4.6 PL Analysis of $10^{15}$ ions/cm<sup>2</sup> Ge Implanted and Annealed GaSe

Fig.4.17 shows PL spectra of GaSe-3A sample in the wavelength range from 570 to 850 nm and temperature between 28 and 90 K. In the spectrum obtained at 28 K,

four peaks at 592.4 nm (2.093 eV, A-band), 605.8 nm (2.046 eV, B-band), 672 nm (1.845 eV, C-band), and 763.7 nm (1.624 eV, D-band) were observed. Although A, B, and C band intensities decreased continuously with increasing sample temperature, intensity of D band showed a little different behavior.

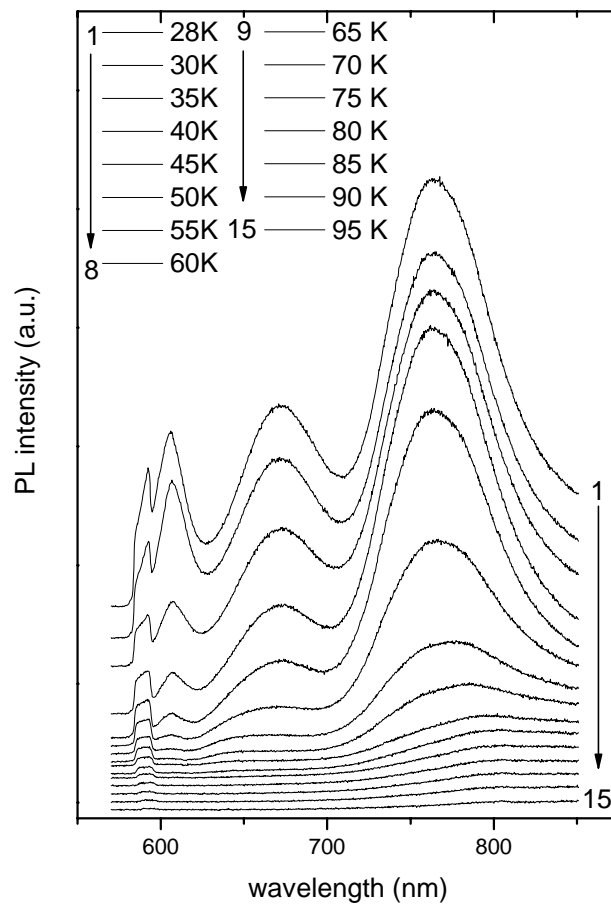


Fig.4.17. Temperature dependence of PL spectra obtained from GaSe-3A

Fig.4.18 gives the semi logarithmic plot of bands intensities as a function of temperature. As shown in the figure, while A, B and C-band intensities decreased slowly until 35 K for B-band and 45 K for A and C bands, above these temperatures the decrease in intensities of the peaks became faster. However, intensity of D-band decreased in the 28-35 K range and except for a very small range of temperatures between 35- 40 K, where it increases, it decreased sharper above 40 K. The small increase in the PL intensity of D-band between 35 and 40 K might result from

changes of the distribution of carriers as the B-band is quenching fastly. Using the straight lines in the 45-90 K, 35-55 K, 45-55 K, and 45-90 K regions, the activation energies of the emission bands were found as 0.020, 0.025, 0.029, and 0.023 eV for A-, B-, C-, and D-band, respectively.

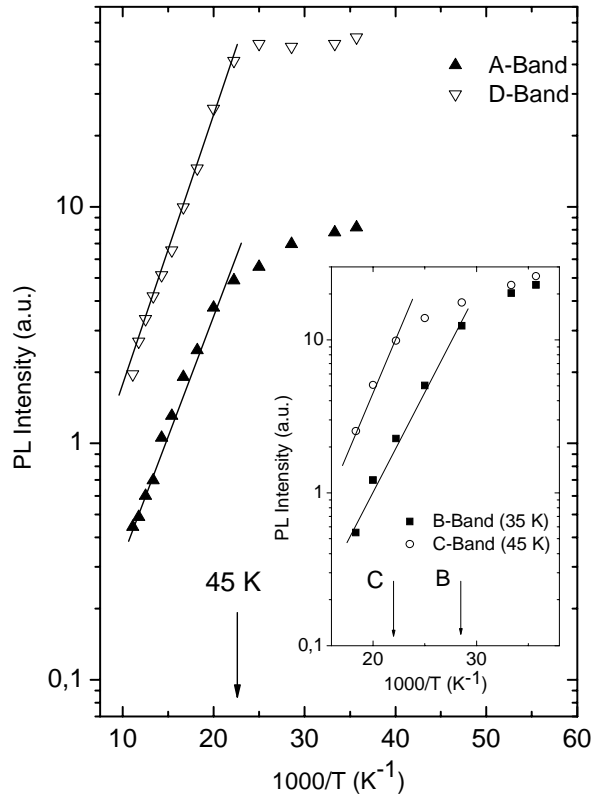


Fig.4.18. The variation of PL intensity of the bands observed in GaSe-3A

Similar to the A bands observed in our other samples, A-band, located at 592.4 nm obtained from GaSe-3A crystal, might be attributed to the radiative recombination of direct free excitons due to the exact agreement between our activation energy result and the value of 0.020 eV given in ref. [24, 25, 28] and very good agreement between the peak center and the values reported in the literature [24, 25, 27, 31, 32]. Direct forbidden energy gap of the GaSe-3A sample was found to be 2.113 eV at 28 K. The activation energy of B, C and D emission bands were donated to the acceptor levels 0.025, 0.029 eV, and 0.023 eV above the top of the conduction band, respectively. As it is stated before, Capozzi has been observed an acceptor level at 0.023 eV [24] and another acceptor at 0.030 eV level has been reported by [29]. It is

seen that the obtained acceptor levels from GaSe-3A sample are in good agreement with the previously obtained results.

A peak located at 603.994 nm has been reported previously by Chung et al. [35] and it has been attributed to indirect bound exciton. However, there has been no information about which phonon has given off during the recombination process. The center of B-band observed from GaSe-3A (605.8 nm) is in very good agreement with this result. Moreover, indirect band gap calculated from the direct gap of the GaSe-3A sample is in fair arrangement with the sum of the peak energy and the activation energy of the sample with a difference of 0.016 eV. This energy might be due to the release of the  $A_1'$  phonon whose energy has been given 0.015 eV in the literature [24]. As a result, it is possible to say that B-band may result from the recombination of the indirect excitons bound to acceptor level at 0.026 eV with emission of an  $A_1'$  phonon.

In order to understand radiative recombination mechanisms, resulting in C and D band emissions, the variations of energy of these two emission bands were given in Fig.4.19. For both peaks, continuous red shifts were observed. The magnitude of energy shifts were 0.016 and 0.095 eV for C and D bands, respectively. Since the decrease in the energies of both bands was different, it is possible to say that the centers responsible for the observed recombinations were not the same. This negative shift of the peaks might be due to donor acceptor transitions [60].

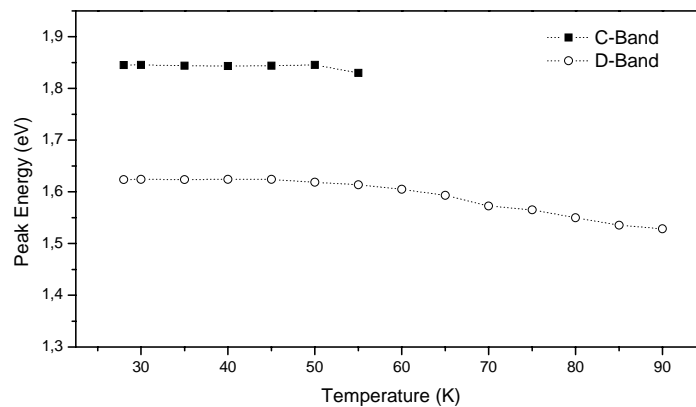


Fig.4.19. Temperature dependence of the C and D band energies

The sum of C-band energy of 1.845 eV and its thermal activation energy of 0.029 eV is smaller than the value of the band gap of the sample. Therefore, if GaSe-3A sample has a donor state centered at 0.239 eV below the conduction band, the recombination mechanism causing C-band might be attributed to the recombination of the electrons located at donor level at 0.239 eV and holes at acceptor level at the 0.029 eV. Similarly, the donor level at located 0.466 eV was obtained for D-emission peak by adding the band energy of 1.624 eV to the thermal activation energy of 0.023 eV and subtracting the found value from the forbidden energy gap of GaSe-3A crystal at 28 K. As a result, it is possible to say D-band might be considered as transitions from the donor level at 0.466 eV to acceptor level located 0.023 eV above the top of the valence band.

Non-excitonic recombination mechanisms for GaSe-3A sample were indicated in Fig. 4.8. Two shallow acceptor levels  $a_1$  and  $a_2$  located at 0.023 and 0.029 eV above the top of the valence band are indicated in the figure. From the analysis of C and D bands, two deep donor levels  $d_1$  and  $d_2$  located at 0.239 and 0.466 eV below the conduction band are calculated and introduced in to direct energy gap of GaSe-3A.

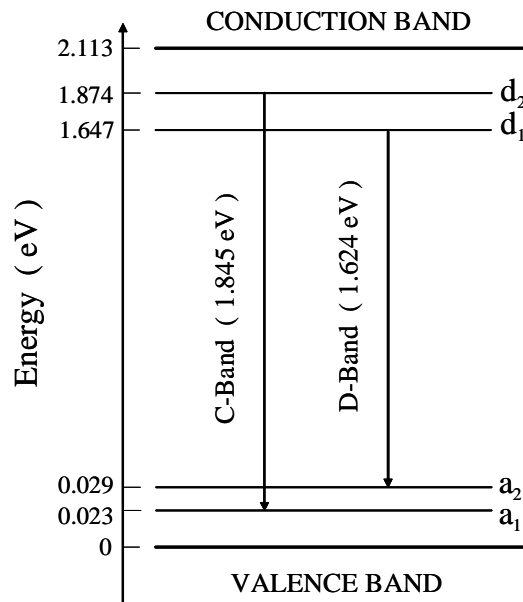


Fig.4.20. The proposed energy band diagram for GaSe-3A sample at 28 K

## 4.7 Comparison of Results Obtained From As Grown and Implanted Samples

PL spectra of unimplanted and Ge implanted GaSe samples at 35 K are indicated in Fig.4.21 for comparison. Direct free excitonic band, labeled as A, is centered at 590.4 nm, 590.2 nm, 594.5 nm and 588.9 nm for GaSe-0, GaSe-1, GaSe-2, and GaSe-3 crystal at 35 K. The activation energy of the peak is found 0.019, 0.020, 0.018, and 0.019 eV, in very good agreement with the reported value of 0.020 eV [24, 25, 27, 31, 32]. Direct forbidden gaps of the samples were found 2.120 eV at 32 K, 2.121 eV at 25 K, 2.121 eV at 21 K, and 2.124 eV at 33 K for GaSe-0, GaSe-1, GaSe-2, and GaSe-3 crystals, respectively. In addition, from GaSe-1 sample, direct exciton bound to an acceptor level located at 0.050 eV above the valence band was observed at 601.8 nm at 35 K and indicated as B-band. Furthermore, an emission peak at 611.3 nm due to indirect free exciton associated with three  $A_1'$  phonons has been observed and labeled as B-band for GaSe-3 sample.

The two peaks observed in the lower part of the spectrum of all samples do not have excitonic origin and may be caused by impurity levels. B-band observed in GaSe-0 sample is centered at 676 nm at 35 K and has activation energy of 0.017 eV. This band may be attributed to the recombination of the electrons located at the donor level at 0.266 eV and holes at the acceptor level of 0.017 eV. C-band at 670.8 nm at 35 K was observed in the spectrum of the GaSe-1 sample. Its activation energy is 0.026 eV and may be due to the transition from the donor level located at 0.243 eV to the acceptor level at 0.026 eV. The middle peak, B-band, observed in the spectrum of GaSe-2 sample has a center of 674.5 nm at 35 K and may be due to donor (at 0.265 eV)-acceptor (0.014 eV) pair recombination. In the spectrum of GaSe-3 crystal, a peak centered at 677.3 nm and with activation energy of 0.033 eV was observed. This band may be considered as transitions from the donor level at 0.256 eV below the conduction band to acceptor level at 0.033 eV above the valence band. In the spectra of all samples, the lowest energy peak is centered at 761.3 nm, 762.1 nm, 765.3 nm, and 763.9 nm at 35 K for GaSe-0, GaSe-1, GaSe-2, and GaSe-3 crystals, respectively. The activation energies of the peaks were found 0.031, 0.028, 0.034,

and 0.025 eV. They may be attributed to donor acceptor pair recombination.

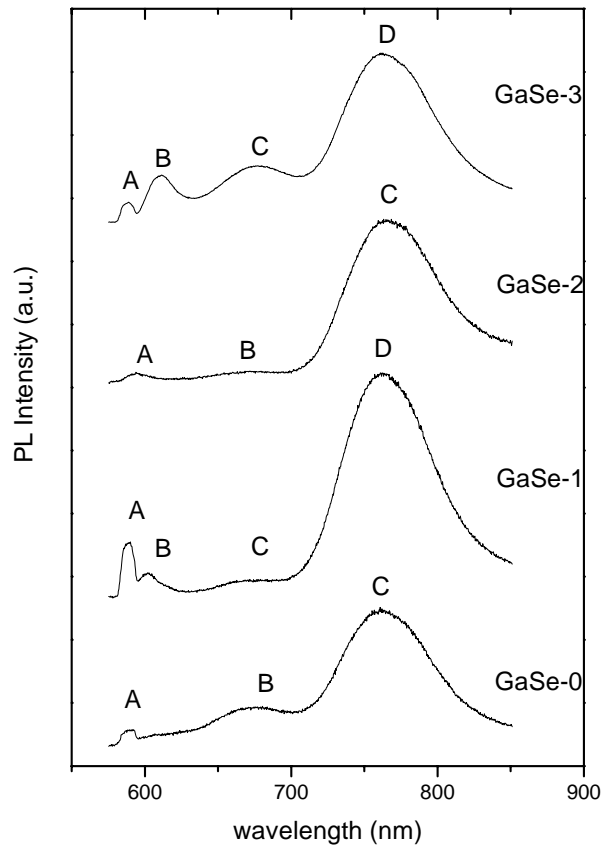


Fig.4.21. PL spectra of unimplanted and Ge-implanted GaSe crystals at 35 K

Obtained non excitonic peak centers and activation energies for all samples are very close to each other. In addition, it is seen that the relative intensities of the all peaks show differences. It has been reported by Matsumura et al. [26] that the PL spectra of GaSe crystals grown by Bridgman method can change with respect to the sample prepared from which part of the ingot (top or bottom), different samples prepared from the top of grown ingot, the point on the sample where laser has been incident. In the study, changes in PL intensities of the peaks and the number of observed peak have been observed with different samples and exciting position [26]. Therefore, we consider that the small variations in the spectra of all samples might not be due to Ge implantation.

In order to see the effect of annealing to the PL spectra of GaSe-3, annealing process was performed at 500 °C for 20 minutes. Fig.4.22 indicates the PL spectrum of the GaSe-3 and GaSe-3A samples at 35 K. Both spectra contain four emission peaks while their locations and impurity levels resulting in these bands shows differences. The centers of peaks observed in GaSe-3 sample were found 588.9 nm, 611.2 nm, 677.3 nm, and 763.9 nm at 35 K and activation energies were 0.019, 0.017, 0.033, and 0.025 eV for A, B, C, and D bands, respectively. In the spectrum of GaSe-3A crystal at 35 K, excitonic bands, A and B bands, were observed at 592.7 nm and 607.7 nm with activation energy of 0.020 eV and 0.025 eV, respectively while impurity related emissions, C and D bands, were centered at 672.6 nm and 763.7 nm with activation energies 0.029 eV and 0.023 eV, respectively. From the direct free excitonic peaks of both spectra, direct energy gaps of the samples were evaluated to be 2.124 and 2.113 eV for GaSe-3 and GaSe-3A, respectively. In addition, it is possible to say that with annealing at 500 °C for 20 minutes defects which sample might contain can not be removed.

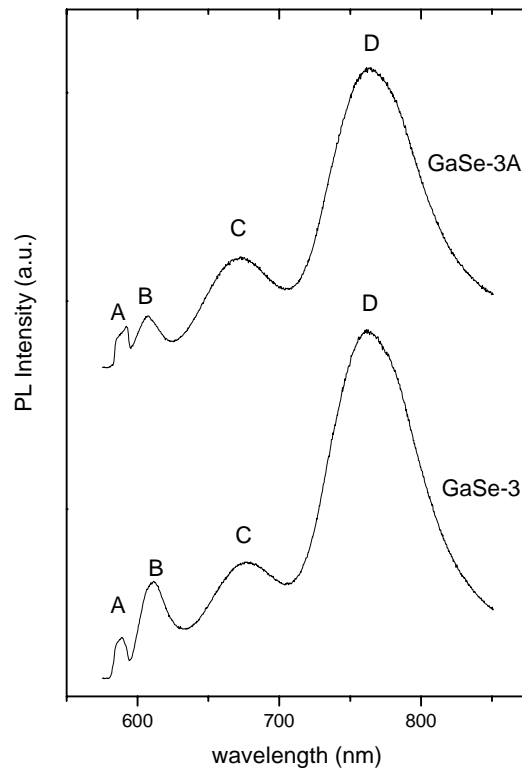


Fig.4.22. PL spectrum of GaSe-3 and GaSe-3A samples at 35 K

## 4.8 PL Properties of InSe Crystals

PL spectrum of as grown (InSe-0),  $10^{13}$  (InSe-1),  $10^{14}$  (InSe-2), and  $10^{15}$  (InSe-3) ions/cm<sup>2</sup> Ge implanted InSe crystals at 20 K is presented in Fig. 4.23 for comparison. In the spectrum of all samples, two broad bands, labeled as A and B, were observed. The center of A-band are observed at 966.6 nm (1.283 eV), 964.7 nm (1.285 eV), 964.4 nm (1.286 eV), and 971.2 nm (1.277eV) while B-band was observed at 990.8 nm (1.251 eV), 990.8 nm (1.251 eV), 992 nm (1.250 eV), and 989.3 nm (1.253 eV) for InSe-0, InSe-1, InSe-2, and InSe-3 samples, respectively.

Direct free excitonic peak for InSe crystal has been observed at 936 nm (1.325 eV), 935.8 nm (1.325 eV), and 1.336 eV by the ref. [48, 49, 63]. In addition, Imai has reported that the emission bands above 932.33 nm (below 1.330 eV) are due to the imperfections such as native defects and/or mechanical damages introduced during the cleavage of the crystal [63]. Therefore, the observed bands may be related to impurities or/and defects introduced during the growth or/and cleaving processes.

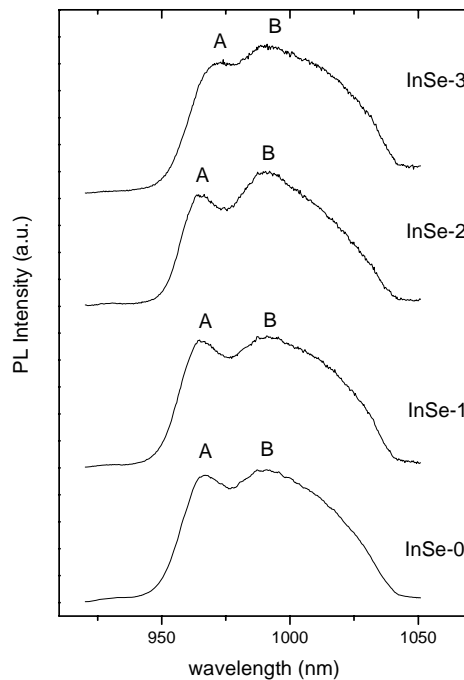


Fig. 2.23 PL spectrum of InSe samples at 20 K

Fig.4.24. displays the PL spectra of InSe-3 and InSe-3A samples at 20 K. It is seen that relative intensity from the emission band B decreases with annealing process. The centers of A and B bands were at 971.2 nm (1.277 eV) and 989.3 nm (1.253 eV), while in the annealed sample, they were observed at 969.3 nm (1.279 eV) and 989.3 nm (1.253 eV), respectively. However, the variation in these values might not be due to annealing effect but might be due to the inhomogeneous sample surface and laser light incident at different points on the surface.

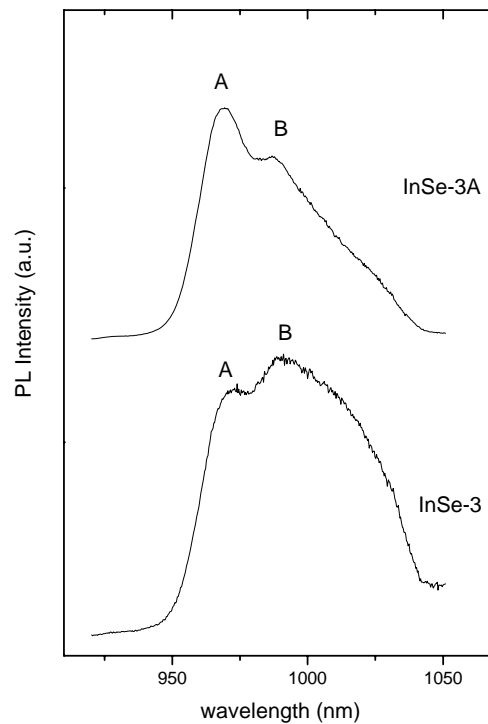


Fig.4.24. PL spectra of InSe-3 and InSe-3A samples at 20 K

## CHAPTER V

### CONCLUSIONS

In this work, low temperature photoluminescence properties of two interesting layered semiconductors GaSe and InSe crystals have been investigated. The crystals have been grown by a 3-zone Vertical Bridgman- Stockbarger system in the Crystal Growth Laboratory of Department of Physics at METU. Firstly, PL measurement has been performed for as grown GaSe crystal. Then, ions of Germanium have been implanted into samples, prepared from the same GaSe ingot, with 100 keV energy and ion doses of  $1 \times 10^{13}$ ,  $1 \times 10^{14}$ ,  $1 \times 10^{15}$  ions/cm<sup>2</sup>. PL measurements have been repeated for these samples. After that, the sample in which  $1 \times 10^{15}$  ions/cm<sup>2</sup> Ge implanted has been annealed at 500°C for 20 minutes in order to see the effect of annealing to the emission spectrum of the sample. The same steps have been performed for InSe crystals. The results obtained from temperature dependent PL spectra of GaSe samples were given in Table 5.1.

As it is stated before, luminescence spectra of GaSe may change considerably from sample to sample. In addition, it is possible to observe different spectra from the same sample by changing exciting position on the surface [26]. Since similar spectra have been observed in this study and the acceptor-donor levels are close the each other, it is possible to say with increasing implantation dose and annealing process, it has not been observed considerable changes in the PL spectrum of the GaSe samples at least in the study range of the spectrum. In the literature, there are many reports

Table 5.1. Obtained PL bands for GaSe samples in this study

Sample name	Band	Center	Activation energy (eV)	Recombination mechanism
As grown GaSe (GaSe-0) (32 K)	A	590.2 nm (2.101 eV)	0.019	Direct free exciton
	B	674.9 nm (1.837 eV)	0.017	Donor (at 0.266 eV) Acceptor (at 0.017 eV) pair transition
	C	759.6 nm (1.632 eV)	0.031	Donor (at 0.457 eV) Acceptor (at 0.031 eV) pair transition
$10^{13}$ ions/cm <sup>2</sup> Ge imp. GaSe (GaSe-1) (25 K)	A	590.2 nm (2.101 eV)	0.020	Direct free exciton
	B	598.8 nm (2.071 eV)	0.049	Direct exciton bound to acceptor at 0.049 eV
	C	668.4 nm (1.855 eV)	0.022	Donor (at 0.243 eV) Acceptor (at 0.022 eV) pair transition
	D	762.5 nm (1.626 eV)	0.028	Donor (at 0.467 eV) Acceptor (at 0.028 eV) pair transition
$10^{14}$ ions/cm <sup>2</sup> Ge imp. GaSe (GaSe-2) (21 K)	A	589.6 nm (2.103 eV)	0.018	Direct free exciton
	B	673.3 nm (1.842 eV)	0.014	Donor (at 0.265 eV) Acceptor (at 0.014 eV) pair transition
	C	764.6 nm (1.622 eV)	0.034	Donor (at 0.465 eV) Acceptor (at 0.034 eV) pair transition
$10^{15}$ ions/cm <sup>2</sup> Ge imp. GaSe (GaSe-3) (33K)	A	588.9 nm (2.105 eV)	0.019	Direct free exciton
	B	610.1 nm (2.032 eV)	0.017	Indirect free exciton with three $A_1'$ phonons
	C	672.8 nm (1.843 eV)	0.025	Donor (at 0.256 eV) Acceptor (at 0.025 eV) pair transition
	D	763.9 nm (1.623 eV)	0.025	Donor (at 0.476 eV) Acceptor (at 0.025 eV) pair transition
$10^{15}$ ions/cm <sup>2</sup> Ge imp. annealed GaSe (GaSe-3A) (28 K)	A	592.4 nm (2.093 eV)	0.020	Direct free exciton
	B	605.8 nm (2.046 eV)	0.025	Indirect excitons bound to acceptor level at 0.026 eV with an $A_1'$ phonon
	C	672 nm (1.845 eV)	0.029	Donor (at 0.239 eV) Acceptor (at 0.029 eV) pair transition
	D	763.7 nm (1.624 eV)	0.023	Donor (at 0.466 eV) Acceptor (at 0.023 eV) pair transition

about PL properties of the various chemically doped GaSe samples [31-36, 38-41]. In these studies, new peak or peaks in the lower energy part of PL of undoped sample

have been observed with doping of the ions and the intensity of the peak has been increased with increasing doping concentration. However, in this study which is implantation but not chemical doping, a new peak resulting from Ge ions has not been observed upon implantation, as the dose is increased and upon annealing.

Since the quantum efficiency of CCD, used in the performed measurements, is very low in the high wavelength region and after 1050 nm we could not see the spectrum, it is possible to say that there may be a new peak or peaks after 1050 nm.

Direct band gap energies of GaSe samples also evaluated from the direct excitonic peak positions and their activation energies. They have been found to be 2.120 eV at 32 K, 2.121 eV at 25 K, 2.121 eV at 21 K, and 2.124 eV at 33 K for GaSe-0, GaSe-1, GaSe-2, and GaSe-3 crystals, respectively.

PL spectrum of as grown InSe,  $1 \times 10^{13}$ ,  $1 \times 10^{14}$ , and  $1 \times 10^{15}$  ions/cm<sup>2</sup> Ge implanted InSe sample at 20 K have been obtained in order to see the PL properties of the InSe samples. Then,  $1 \times 10^{15}$  ions/cm<sup>2</sup> Ge implanted InSe has been annealed at 500 °C for 20 minutes. It has been observed two peaks from all InSe samples at about the same centers and considered that they may be impurity related emissions. In the spectrum of all InSe samples, there has not been observed excitonic peaks. The reason may be the damages introduced by the growth and or cleaving. In addition, because the centers and relative intensities of all peaks are very close to each other, it is possible to say that it has not been observed considerable changes resulting from implantation. Moreover, because quantum efficiency of CCD is very low at about 1000 nm, it should be noted that reliability of center of low energy band observed in the spectrum of all InSe samples is low.

## REFERENCES

- [1] K. Seeger, “*Semiconductor Physics an Introduction*”, 7th ed., Berlin ; Springer, (1999)
- [2] B. G. Yacobi, “*Semiconductor Materials*”, Kluwer Academic/Plenum Publishers, Newyork, Boston, Dordrecth, London, Moscow, (2002)
- [3] Ben G. Streetman, “*Solid State Electronic Devices*”, Prentice- Hall, New Jersey, (1995)
- [4] Subash Mahajan, K.S. Sree Harsha, “*Principles of Growth and Processing of Semiconductors*”, McGraw-Hill Series in Materials Science and Engineering, (1999)
- [5] Donald A., Neamen “*Semiconductor Physics & Devices*”, 3rd ed., Boston : McGraw-Hill, (2003)
- [6] J. V. McCanny and R.B.Murray, J. Phys. C: Sol. Stat. Phys., 10, 1211, (1977)
- [7] M. Khalid Anis, F.M.Nazar, J. Mater. Sci. Lett. 2, 471, (1983)
- [8] Y. Depeursinge, Nuovo Cimento, 64B, 111, (1981)
- [9] G. Fischer and J.L.Brebner, J. Phys. Chem. Solids, 23, 1363 (1962)
- [10] Z. S. Basinski, D. B. Dove and E. Mooser, Helv. Phys. Acta, 34, 373, (1961)
- [11] M. Schluter, Nuovo Cimento, 13B, 313, (1972)
- [12] F. Bassani and G. Pastori Parravicini, Nuovo Cimento, LB, 95, (1966)
- [13] C. Ulrich, D. Olguin, A. Cantarero, A.R.Goni, K. Syassen and A. Chevy, Phys. Stat. Sol.(b), 221, 777, (2000)
- [14] J. Roberts, J. Phys.C: Sol. Stat. Phys., 12, 4777, (1979)
- [15] A. Gousskov, J. J. Camasell and L. Gousskov, Prog. Cryst. Growth Charact. Mater., 5, 323, (1982)
- [16] A. Kuhn and R. Chevalier and A. Rimsky, Acta Cryst. B31, 2841, (1975)
- [17] J. C. J. M. Terhell, Prog. Cryst. Growth Charact. Mater., 7, 55, (1983)
- [18] A. Kuhn, A. Chevy and R. Chevalier, Phys. Stat. Sol. (a), 31, 469, (1975)
- [19] Y. Depeursinge, E. Doni, R. Girlanda, A. Baldereschi and K. Maschke, Sol. Stat. Commun., 27, 1449, (1978)

- [20] A. Mercier, E. Mooser, and J. P. Voitchovsky, *Phys. Rev. B*, 12, 4307, (1975)
- [21] M. O. D. Camara and A. Mauger, I. Devos, *Phys. Rev. B*, 65, 125206, (2002)
- [22] N.C. Fernelius, *Prog. Cryst. Growth Charact. Mater.*, 28, 275, (1994)
- [23] A. Seyhan, O. Karabulut, B. G. Akınoğlu, B. Aslan, and R. Turan, *Cryst. Res. Technol.*, 40, 893, (2005)
- [24] V. Capozzi, *Phys. Rev. B*, 23, 836, (1981)
- [25] J. P. Voitchovsky and A. Mercier, *Nuovo Cimento B*, 22, 273, (1974)
- [26] T. Matsumura, *Phys. Stat. Sol. (a)*, 43, 685, (1977)
- [27] I. I. Dobynde, A. I. Bobrysheva, I. M. Razdobreev, and Yu. G. Shekun, *Phys. Stat. Sol. (b)*, 147, 717, (1988)
- [28] V. Capozzi, S. Caneppele, M. Montagna, and F. Levy, *Phys. Stat. Sol. (b)* 129, 247, (1985)
- [29] V. Capozzi and M. Montagna, *Phys. Rev. B*, 40, 3182, (1989)
- [30] A. Aydinli, N. M. Gasanly, and K. Goksen, *Philos. Magazine Lett.*, 81, 859, (2001)
- [31] S. Shigetomi, T. Ikari, and H. Nakashima *J. Appl. Phys.* 74, 4125, (1993)
- [32] V. Capozzi, *Phys. Rev. B*, 28, 4620, (1983)
- [33] S. Shigetomi, T. Ikari, and H. Nakashima *J. Appl. Phys.* 69, 7936, (1991)
- [34] S. Shigetomi and T. Ikari, *Philos. Magazine Lett.*, 79, 575, (1999)
- [35] C. H. Chang, S. R. Hahn, H. L. Park, W. T. Kim, and S. I. Lee, *J. Luminescence*, 40&41, 405, (1988)
- [36] Chang-Dae Kim, Ki-Wan Jang, Yong-Il Lee, *Solid Stat. Commun.* 130, 701, (2004)
- [37] S. Shigetomi and T. Ikari, *J. Appl. Phys.*, 95, 6480, (2004)
- [38] S. Shigetomi and T. Ikari, *Phys. Stat. Sol. (b)* 242, 3123, (2005)
- [39] S. Shigetomi, T. Ikari, and H. Nakashima, *Phys. Stat. Sol. (a)* 160, 159, (1997)
- [40] S. Shigetomi, T. Ikari, and H. Nakashima, *J. Luminescence* 79, 79, (1998)
- [41] Y. K. Hsu, C. S. Chang, W. F. Hsieh, *Jpn. J. Appl. Phys.* 1 42, 4222, (2003)

- [42] S. Shigetomi, T. Ikari, H. Nakashima, *Jpn. J. Appl. Phys.* 1 35, 429, (1996)
- [43] S. Shigetomi, T. Ikari, H. Nakashima *Phys. Stat. Sol. (a)*, 156, K21, (1996)
- [44] A. Sh. Abdinov, R. F. Babaeva, R. M. Rzaev, and G. A. Gasanov, *Inorganic Materials*, Vol. 40, 660, (2004)
- [45] S. Shigetomi, T. Ikari, and H. Nakashima, *Phys. Stat. Sol. (a)*, 185, 341, (2001)
- [46] V. Capozzi and A. Minafra, *Sol. Stat. Commun.*, 38, 341, (1981)
- [47] G. A. Akhundov, I. B. Ermolovich. F. N. Kaziev, and K. Sheinkman, *Phys. Stat. Sol.* 35, 1065, (1969)
- [48] L. N. Kurbatov, A. I. Dirochka, V. L. Bakumenko, and Z. D. Kovalyuk, *Sov. Phys.-Sol. Stat.*, 12, 2956, (1971)
- [49] V. L. Bakumenko, Z. D. Kovalyuk, L. N. Kurbatov, D. V. Sobolev, and V. F. Chishko, *Sov. Phys. Semicond.*, 8, 660, (1974)
- [50] K. Imai, K. Suzuki, T. Haga, and Y. Abe, *J. Appl. Phys.* 60, 3374, (1986)
- [51] B. Abay, H. Efeoglu, and Y. K. Yogurtcu, *Mater. Research Bullet.*, 33, 1401, (1998)
- [52] J. Camassel, P. Merle, H. Mathieu, and A. Chevy, *Phys. Rev. B*, 17, 4718, (1978)
- [53] S. Shigetomi, T. Ikari, and H. Nakashima, *Phys. Stat. Sol. (b)*, 209, 93, (1998)
- [54] S. Shigetomi and T. Ikari, *Phys. Stat. Sol. (b)*, 236, 135, (2003)
- [55] S. Shigetomi and T. Ikari, *J. Appl. Phys.*, 93, 2301, (2003)
- [56] S. Shigetomi, T. Ikari, *Jpn. J. Appl. Phys.* 1 42, 6951, (2003)
- [57] J. Riera, A. Segura, A. Chevy, *Phys. Stat. Sol. (a)*, 142, 265, (1994)
- [58] S. Shigetomi, H. Ohkubo, and T. Ikari, *J. Phys. Chem. Solids*, 51, 91, (1990)
- [59] V. V. Gridin, C. Kasl, J. D. Comins, and R. Beserman, *J. Appl. Phys.* 71, 6069, (1992)
- [60] S. Shigetomi, T. Ikari, and H. Nakashima, *J. Appl. Phys.* 76, 310, (1994)
- [61] B. G. Tagiev, G. M. Niftiev, and S. A. Abushov, *Phys. Stat. Sol. (b)*, 121, K195, (1984)
- [62] K. Imai, K. Suzuki, T. Haga, and Y. Abe, *J. Appl. Phys.* 60, 3374, (1986)

- [63] K. Imai, J. Luminescence 43, 121, (1989)
- [64] Subash Mahajan, K. S. Sree Harsha, “*Principles of Growth and Processing of Semiconductors*”, McGraw-Hill Series in Material Science and Engineering, (1999)
- [65] S.M. Sze, “*VLSI Technology*”, New York : McGraw-Hill, (1988)
- [66] B. R. Pumphlin, “*Crystal Growth*“, Pergamon Press Ltd., Headington Hill Hall, Oxford, (1975)
- [67] J. C. Brice, ‘*The Crystal Growth of Crystals from Liquids*’ Amsterdam, North-Holland Pub. Co.; New York, American Elsevier, (1973)
- [68] H. Xiao, “*Introduction to Semiconductor Manufacturing Technology*”, Prentice-Hall Inc., New Jersey, (2001)
- [69] C. H. L. Goodman, ‘*Crystal Growth: Theory and Techniques*’ London ; New York : Plenum Press, (1974)
- [70] S. M. Sze, “*Semiconductor Devices, Physics and Technology*” New York:Wiley, (1985)
- [71] James W. Mayer, Lennart Eriksson and John A. Davies, “*Ion implantation in semiconductors, silicon and germanium*” New York, Academic Press, (1970)
- [72] Leverenz, H. W. An Introduction to Luminescence of Solids, Dover Publications, New York. (1968).
- [73] A.M. García-Campaña and W.R.G. Baeyens, Luminescence Spectr., 28, 686, (2000)
- [74] Peter Y. Yu, Manuel Cardona, “*Fundamentals of Semiconductors*” New York, Springer, (2001)
- [75] Richard H. Bube, “*Photoconductivity of Solids*”, New York, Wiley, (1960)
- [76] Sidney Perkowitz, “*Optical Characterization of Semiconductors*”, London, San Diego : Academic Press, (1993)
- [77] Bebb, H. B. and Williams, E. W, ‘*Semiconductors and Semimetals*’, edited by R. K. Willardson and A. C. Beer Academic, New York, (1966)
- [78] Jacques I. Pankove, “*Optical Processes in Semiconductors*”, Englewood Cliffs, N.J., Prentice-Hall, (1971)
- [79] Dieter K. Schroder, “*Semiconductor Material and Device Characterization*” New York : Wiley, (1998)
- [80] Taguchi T., Shirafuji, and Inuishi Y., Phys. Stat. Sol. (b), 68, 727, (1975)

- [81] Kim Q., and Langer D. W., Phys. Stat. Sol. (b), 122, 263, (1984)
- [82] Schmidt, T., K. Lischka, and W. Zulehner, Phys. Rev. Lett., B45, 8989, (1992)
- [83] Varshni Y. P., Physica, 34, 149, (1967)
- [84] Leroux M., Grandjean N., Beurnout B., Nataf G., Sernond F., Massies J., and Gibart P., J. Appl. Phys., 89, 3720, (1999)
- [85] Kim J. C., Rho H., Smith L. M., Jackson H. E., Dobrowolska M., Lee S., Furdyna J. K., Appl. Phys. Lett., 75, 214, (1999)
- [86] Zubrilov A. S., Nikishin S. A., Kipshidze G. D., Kuryatkov V. V., and Temkin H., T. Prokofyeva I. and Holtz M., J. Appl. Phys., 91, 1209, (2001)
- [87] E. W. Williams and R. Hall '*Luminescence and the light emitting diode*', New York : Pergamon Press, (1978)
- [88] V. L. Cardetta, A. M. Mancini, and A. Rizzo, J. Cryst. Growth, 16, 185, (1972)
- [89] H. Karaagac, '*Structural, Electrical and Optical Characterization of Ge-implanted GaSe Single Crystal Grown by Bridgman Method*', M. Sc. Thesis, METU, Ankara, (2005)
- [90] D. Deniz, '*Growth and Characterization of InSe Single Crystals*', M. Sc. Thesis, METU, Ankara, (2004)
- [91] Crystalox, "*MD4000 Operation Manual*", Crystalox Com., (1994)
- [92] Manual of CTI-Cryogenics M-22" Closed-Cycle Helium Cryostat, Cryophysics
- [93] User's Manual, Model 330 Autotuning Temperature Controller, LakeShore Measurement and Control Technologies, (1992)
- [94] Instruction Manual, MS257<sup>TM</sup> Monochromator and Spectograph Model 777700a, ORIEL Instruments
- [95] Instruction Manual, C7040/C7041/C7042, MultiChannel Detector Head with Back-Tinned CCD, Hamamatsu Solid State Division
- [96] J. L. Brebner Phys. Lett., 24A, 274, (1967)
- [97] C. Manfredotti, R. Murri, A. Rizzo, S. Galassini, and L. Ruggiero, Phys. Rev. B, 10, 3387, (1974)
- [98] PH. Schmid, J. P. Voitchovsky, and A. Mercier , Phys. Stat. Sol. (a), 21, 443, (1974)
- [99] G. Micocci, A. Serra, and A. Tepore, Phys. Stat. Sol. (a), 162, 64, (1997)

[100] T. W. Kang, S. H. Park, H. Song, T. W. Kim, G. S. Yoon, and C. O. Kim, *J. Appl. Phys.*, 84, 4, (1998)

[101] N. M. Gasanly, A. Aydinli, A. Bek, and I. Yilmaz, *Solid Stat. Commun.*, 105, 21, (1998)

[102] K. Goksen, N. M. Gasanly, A. Seyhan, R. Turan, *Mater. Sci. and Engineering, B*, 127, 41, (2006)

[103] A. Aydinli, N. M. Gasanly, I. Yilmaz and A. Serpenguzel *Semicond. Sci. Technol.*, 14, 599, (1999)